M 2024

U.PORTO
FEUP FACULDADE DE ENGENHARIA
UNIVERSIDADE DO PORTO

# CHARACTERIZATION OF ORGANIC-ACID-BASED AQUEOUS TWO-PHASE SYSTEMS FOR CRITICAL METAL SEPARATION

**BRUNA RODRIGUES CINTRA**

MASTER THESIS IN CHEMICAL ENGINEERING
PRESENTED TO THE FACULTY OF ENGINEERING
OF THE UNIVERSITY OF PORTO

Master in Chemical Engineering

# *Characterization of organic-acid-based aqueous two-phase systems for critical metal separation*

## Master Thesis

of

**Bruna Rodrigues Cintra**

**Developed within the course of dissertation**

held in

**Associate Laboratory LSRE-LCM**

SRE CM ASSOCIATE LABORATORY
LABORATORY OF SEPARATION AND REACTION ENGINEERING
LABORATORY OF CATALYSIS AND MATERIALS

Supervisor at FEUP: **Prof. Helena Passos**

Joint supervisor(s) at FEUP: **Prof. Maria Eugénia Macedo**

U.PORTO
FEUP FACULDADE DE ENGENHARIA
UNIVERSIDADE DO PORTO

DEPARTAMENTO DE
ENGENHARIA QUÍMICA

**July 2024**

# Acknowledgment

I would like to extend my sincere gratitude to all those who contributed to completing this work. First and foremost, I am very grateful to have Prof. Helena Passos as my supervisor, I would like to thank you for the invaluable guidance, encouragement, and expertise throughout the research process. Her availability at any time, unwavering support, and belief in my capabilities gave me the strength to persevere, even during challenging times.

I am also deeply grateful to Flávia Braga for her support, collaboration, and our lunch breaks while working together. Special thanks for her assistance with the experimental work and data analysis, which was crucial for the successful execution of this research.

I would like to thank Pedro Velho for his help with the laboratory equipment and his readiness to solve any technical issues that occurred during the research. To my co-supervisor Prof. Maria Eugénia Macedo, for always being available and for her knowledge.

Finally, I am profoundly grateful to my family, they are the ones who give me strength every day making my pathway in life so much easier. Thank you, Mom and Dad, for making any idea of mine come true, for giving me the freedom to do what feels right in the moment for me, for the support when I doubt myself, for everything. A special thanks to my friends for giving me good times, where I can forget for a minute that I have responsibilities. A special thanks to my roommates who turned into friends, Márcia e Osvaldo, for the knowledge, laughter, support, and for making coming to Porto unforgettable.

This work would not have been possible without the contributions and support of all those mentioned above. Thank you for being a part of this journey and for helping me achieve my personal and academic goals.

# Abstract

In this study, the liquid-liquid equilibrium of aqueous two-phase systems (ATPS) composed of organic acids and ionic liquids (IL) was evaluated aiming to develop more efficient and environmentally sustainable hydrometallurgical processes for the recovery of critical metals from secondary sources. The primary objective was to evaluate the possibility of using organic acids in the formation of two liquid phases systems in the presence of IL, evaluating the role of organic acids in phase separation. After the determination of the phase diagrams, the potential use of these ternary systems on critical metals partition and separation was also aimed for.

The solubility curves of ternary systems composed of tributyltetradecylphosphonium chloride ($[P_{44414}]Cl$) IL, six different carboxylic acids (formic, acetic, propionic, butyric, lactic and citric acids), and water, were determined at (298 $\pm$ 1) K and atmospheric pressure. The impact of organic acid nature and temperature on the liquid-liquid separation were evaluated and discussed. The comparison of these systems with their salt-based counterparts was also carried out. Finally, the possibility to develop hybrid quaternary systems, consisting of the mixture of IL, acid, salt and water was evaluated.

A preliminary test on copper partition behavior in a quaternary system composed of $[P_{44414}]Cl$ + citric acid + potassium citrate + water was carried-out. The result indicated that only 14.3% of Cu was partitioned into the IL-rich phase, suggesting that further research and optimization are needed in the design of citric-acid-based quaternary systems for effective metal extraction and separation.

The results obtained in this work show that organic-acid-based ATPS present a complex mechanism of formation and further studies and optimization are required to find a solution for their application on metals separation and mostly for their integration in metals recycling processes.



**Keywords:** Liquid-Liquid Equilibrium, Aqueous Two-Phase Systems, Organic Acids, Recycling, Critical Metals

# Resumo

Neste estudo, o equilíbrio líquido-líquido de sistemas aquosos bifásicos (ATPS, do inglês "Aqueous Two-Phase Systems") compostos por ácidos orgânicos e líquidos iónicos (IL, do inglês "Ionic Liquid") foi avaliado com o objetivo de desenvolver processos hidrometalúrgicos mais eficientes e ambientalmente sustentáveis para a recuperação de metais críticos de fontes secundárias. O principal objetivo foi avaliar a possibilidade de utilizar ácidos orgânicos na formação de sistemas de duas fases líquidas na presença de um líquido iónico, através do estudo do efeito do ácido orgânico na separação de fases. Após a determinação dos diagramas de fase, pretendeu-se também avaliar o potencial uso destes sistemas ternários na partição e separação de metais críticos.

As curvas binodais de sistemas ternários compostos pelo IL cloreto de tributiltetradecilfosfónio ($[P_{44414}]Cl$), seis diferentes ácidos carboxílicos (ácidos fórmico, acético, propiónico, butírico, láctico e cítrico) e água foram determinadas. O impacto do ácido orgânico e da temperatura na separação líquido-líquido foi avaliado e discutido. A comparação destes sistemas com os seus equivalentes à base de sal também foi realizada. Finalmente, foi avaliada a possibilidade de desenvolver sistemas quaternários híbridos, a partir da mistura de IL, ácido, sal e água.

Um teste preliminar sobre o comportamento da partição do cobre num sistema quaternário composto por $[P_{44414}]Cl$ + ácido cítrico + citrato de potássio + água foi realizado. O resultado indicou que apenas 14,3 % do Cu foi extraído para a fase rica em IL, sugerindo que são necessários mais estudos e otimizações no projeto de sistemas quaternários à base de ácido cítrico para a extração e separação eficaz de metais.

Os resultados obtidos neste trabalho mostram que os ATPS à base de ácidos orgânicos apresentam um mecanismo de formação complexo e são necessários estudos mais aprofundados e otimizações para encontrar uma solução para a sua aplicação na separação de metais e, principalmente, para a sua integração em processos de reciclagem de metais.



**Palavras-chave:** Equilíbrio Líquido-Líquido, Sistemas Aquosos Bifásicos, Ácidos Orgânicos, Reciclagem, Metais Críticos

# Declaration

I hereby declare, under word of honor, that this work is original and that all non-original contributions is indicated, and due reference is given to the author and source

*Bruna Cintra, July 1st, 2024*



# Index

**1. Introduction ..... 1**
**1.1. Framing and presentation of the work ..... 1**
**1.2. Contribution of the author to the work ..... 1**
**1.3. Organization of the dissertation ..... 2**
**2. Context and State of the art ..... 3**
**2.1. Critical metals recovery from e-waste ..... 3**
**2.2. Organic acids as alternative leaching reagents ..... 5**
**2.3. Acidic aqueous two-phase systems ..... 6**
2.3.1. Effect of ionic liquid and acid in acidic aqueous two-phase systems ..... 7
2.3.2. Temperature impact ..... 8
2.3.3. Metal partition ..... 8
**3. Materials and Methods ..... 9**
**3.1. Materials and Instrumentation ..... 9**
3.1.1. Materials ..... 9
**3.2. Liquid-liquid equilibria ..... 10**
3.2.1. Determination of tie-lines and tie-line length ..... 10
3.2.2. In-phase water and $Cl^-$ anion quantification ..... 11
3.2.3. Determination of aggregate size ..... 11
3.2.4. Cu partition and quantification ..... 11
**4. Results and Discussion ..... 12**
**4.1. The effect of carboxylic acids ..... 12**
**4.2. Acid vs salt-based aqueous two-phase systems ..... 15**
**4.3. Temperature effect ..... 16**
**4.4. Merchuk equation and tie-lines determination ..... 17**
**4.5. Phase diagrams of quaternary mixtures ..... 18**
**5. Conclusion ..... 22**
**6. Assessment of the work done ..... 23**
**6.1. Objectives Achieved ..... 23**
**6.2. Contribution to the Sustainable Development Goals ..... 23**
**6.3. Final Assessment ..... 25**
**7. References ..... 26**
**Appendix A – Solubility curves data ..... 33**

**A.1 Experimental solubility data for systems composed of $[P_{44414}]Cl$ + acid + $H_2O$..... 33**
**A.2 Experimental solubility data for systems composed of $[P_{44414}]Cl$ + salt + $H_2O$ ..... 37**
**A.3 Experimental solubility data for systems composed of $[P_{44414}]Cl$ + acid + salt + $H_2O$ 40**
**Appendix B – Copper calibration curve ..... 42**

# List of Figures

*Figure 1 - Critical raw materials technological applications and their current supply risks [7]. ..... 4*

*Figure 2 – Chemical structure of the IL evaluated in this work: (A) $[P_{4444}]Cl$; (B) $[P_{44414}]Cl$. ..... 9*

*Figure 3 - Evaluation of the carboxylic acid nature impact in the ternary phase diagrams composed of $[P_{44414}]Cl$ + organic acid + water. Experimental data for the acetic acid binodal curve were previously reported and are used here for comparison purposes [2]. ..... 13*

*Figure 4 - Comparison between acid- and salt-based ATPS composed of $[P_{44414}]Cl$ and (A) potassium citrate (●) or citric acid (■); (B) sodium acetate (●) or acetic acid (■); (C) sodium formate (●) or formic acid (■). (D) The influence of salt on ATPS composed of $[P_{44414}]Cl$. ..... 16*

*Figure 5 - The temperature effect on citric-acid-based ATPS: 298 K (●); 323 K (■)..... 17*

*Figure 6 - Phase diagram for the ternary system composed of $[P_{44414}]Cl$ + $K_3C_6H_5O_7$+ $H_2O$, at 298 K and atmospheric pressure: solubility curve data (●), TL data (■), adjusted solubility data through Eq. (1) (−). ..... 18*

*Figure 7 - Liquid-liquid equilibria of quaternary and ternary systems composed of $[P_{44414}]Cl$, $K_3C_6H_5O_7$, $C_6H_8O_7$, and $H_2O$: $[P_{44414}]Cl$ + $K_3C_6H_5O_7$ + $H_2O$ (●); $[P_{44414}]Cl$ + $K_3C_6H_5O_7$ + 5 m% $C_6H_8O_7$ + $H_2O$ (◆); $[P_{44414}]Cl$ + 5 m% $K_3C_6H_5O_7$ + $C_6H_8O_7$ + $H_2O$ (◢); $[P_{44414}]Cl$ + $C_6H_8O_7$ + $H_2O$ (■). ..... 19*

*Figure 8 - The effect of (A) citric acid (at a fixed concentration of 20 m% of IL) and (B) $[P_{44414}]Cl$ (at a fixed concentration of 5 m% of acid) concentration on average aggregate diameter present in $[P_{44414}]Cl$ + $C_6H_8O_7$ + 5 m% $K_3C_6H_5O_7$ + $H_2O$. ..... 20*

*Figure 9 –The UV-vis spectra of Cu on top (blue) and bottom (green) phases of the system $[P_{44414}]Cl$ + $C_6H_8O_7$ + $K_3C_6H_5O_7$ + $H_2O$..... 21*

*Figure B1 - Calibration curve for copper at λ = 817 nm. ..... 42*

# List of Tables

*Table 1 - Fifth list 2023 of Critical Raw Materials for the EU [5].* ..... 3

*Table 2 - Carboxylic acids used in this work and their properties.* ..... 9

*Table 3 – Summary of the ternary mixtures evaluated and their ability to induce (✓) or not (X) the formation of a biphasic system.* ..... 12

*Table 4 – pH, water content, and chloride anion concentration on both IL- and acid-rich phases of systems composed of $[P_{44414}]Cl$ + formic or butyric acid + $H_2O$.* ..... 14

*Table 5 - A, B, and C parameters and correlation coefficients, $R^2$, obtained for ATPS composed of $[P_{44414}]Cl$ + salt + $H_2O$ at 298 K.* ..... 17

*Table 6 - Mass fraction percentage (m%) for the coexisting phases of the systems $[P_{44414}]Cl$ + $K_3C_6H_5O_7$ + $H_2O$, and respective values of TLL, and pH values of each phase.* ..... 18

*Table 7 - Contribution to the SDGs - SDGs applied in this report [59].* ..... 23

*Table A1- Experimental mass fraction percentage data for the systems composed of $[P_{44414}]Cl$ + $C_6H_8O_7$ + $H_2O$ and 298 K and 323 K and atmospheric pressure.* ..... 33

*Table A2- Experimental mass fraction data for the systems composed of $[P_{44414}]Cl$ + $C_3H_6O_3$ + $H_2O$ at 298 K and atmospheric pressure.* ..... 33

*Table A3- Experimental mass fraction percentage data for the systems composed of $[P_{44414}]Cl$ + $C_3H_6O_2$ + $H_2O$ at 298 K and atmospheric pressure.* ..... 34

*Table A4- Experimental mass fraction percentage data for the systems composed of $[P_{44414}]Cl$ + $C_4H_8O_2$ + $H_2O$ at 298 K and atmospheric pressure.* ..... 35

*Table A5- Experimental mass fraction percentage data for the systems composed of $[P_{44414}]Cl$ + $CH_2O_2$ + $H_2O$ at 298 K and atmospheric pressure.* ..... 36

*Table A6- Experimental mass fraction percentage data for the systems composed of $[P_{44414}]Cl$ + $K_3C_6H_5O_7$ + $H_2O$ at 298 K and atmospheric pressure.* ..... 37

*Table A7 - Experimental mass fraction percentage data for the systems composed of $[P_{44414}]Cl$ + $NaC_2H_3O_2$ + $H_2O$ at 298 K and atmospheric pressure.* ..... 38

*Table A8 - Experimental mass fraction percentage data for the systems composed of $[P_{44414}]Cl$ + $NaCHO_2$ + $H_2O$ and 298 K and atmospheric pressure.* ..... 39

*Table A9 - Experimental mass fraction data for the systems composed of $[P_{44414}]Cl$ + $C_6H_8O_7$ + $K_3C_6H_5O_7$ (5 m%) + $H_2O$ and 298 K at atmospheric pressure.* ..... 40

*Table A10- Experimental mass fraction percentage data for the systems composed of $[P_{44414}]Cl$ + 5 m% $C_6H_8O_7$ + $K_3C_6H_5O_7$ + $H_2O$ and 298 K at atmospheric pressure.* ..... 41

# Notation and Glossary

| | |
|---|---|
| $[P_{4444}]Cl$ | Tetrabutylphosphonium chloride |
| $[P_{44414}]Cl$ | Tributyltetradecylphosphonium chloride |
| $pK_a$ | Dissociation constant |
| $\log(K_{ow})$ | Octanol-water partition coefficient |
| $R^2$ | Correlation coefficient |

*Greek Letters*

| | |
|---|---|
| α | ratio between the mass of the IL-rich phase and the total mass of the mixture |

*Indexes*

| | |
|---|---|
| IL | IL-rich phase |
| Salt | Salt-rich phase |
| M | Mixture |

***List of Acronyms***

| | |
|---|---|
| IL | Ionic Liquid |
| WEEE | Waste Electrical and Electronic Equipment |
| AcATPS | Acidic Aqueous Two-Phase Systems |
| ATPS | Aqueous Two-Phase Systems |
| LCST | Lower Critical Solution Temperature |
| UCST | Upper Critical Solution Temperature |
| TL | Tie-line |
| TLL | Tie-line length |

# 1. Introduction

## 1.1. Framing and presentation of the work

The primary focus of this research was developing and characterizing novel acidic aqueous two-phase systems (AcATPS) by using organic acids for the selective separation of critical and strategic metals from electronic waste. The study addresses the urgent need for sustainable and efficient hydrometallurgical approaches within the framework of global environmental remediation. Despite peak mining rates for most metals, the recovery from electronic waste, known as urban ores, remains significantly low [1]. This research proposes a potential solution by the application of organic acids instead of the more aggressive and toxic commonly used inorganic acids.

The use of organic acids as viable leaching agents has already been demonstrated in the literature [2], and here their potential as phase-forming compounds of two-liquid phase systems is evaluated to reach the selective separation of critical and strategical metals.

This research plan involves engaging in several key activities, including cloud-point titration to obtain phase diagrams, and the study of biphasic systems to understand the liquid-liquid equilibria within ternary systems including different combinations of organic acids, ionic liquids (ILs), and water. It also investigated the impact of temperature on phase equilibria. The development of hybrid systems – quaternary mixtures composed of IL, acid, salt, and water – was also evaluated.

Once the phase diagrams were characterized, a preliminary test on the distribution of specific metals was carried-out. Through this analysis, we aim to better understand how effectively these systems can separate metals.

## 1.2. Contribution of the author to the work

In this work, the liquid-liquid equilibria of ternary systems composed of an IL, different organic acids, and water were determined to infer on the impact of organic acids in the formation of acid ATPS. These systems play a crucial role in creating alternative, environmentally friendly hydrometallurgical processes for recovering essential metals from waste. In addition to experimentally determined solubility curves, significant progress has been made in comprehending the mechanisms behind the formation of these systems, as well as in the development of hybrid systems that incorporate both salts and acids. All this work was carried out by me under the guidance of my supervisors.

## 1.3. Organization of the dissertation

This dissertation is divided into six distinct chapters. Chapter 1, the introduction, explains the motivation behind this work. In Chapter 2, the state of the art, the most important concepts for understanding the importance of this thesis are explored, namely ATPS and their use in metal separation. Chapter 3 details the experimental procedures used in this work, such as the cloud point titration method, and the equations used for experimental data correlation and tie-lines determination. The results obtained in this work are presented in Chapter 4, while the conclusions are summarized in Chapter 5. Chapter 6 highlights the achieved objectives, the limitations encountered, and the proposed future work.

# 2. Context and State of the art

## 2.1. Critical metals recovery from e-waste

Metals are part of our daily lives, yet their significance often goes unrecognized. End-of-life recycling rates for many metals are currently very low, which has significant implications for energy use and resource availability [3]. Utilizing secondary (recycled) sources in metal production, rather than primary sources, helps mitigate future supply concerns related to these non-renewable resources. Increasing the recycling rates of metals can thus play a critical role in promoting sustainability and resource efficiency [1].

The growing request for metals cannot be satisfied solely through recycling. Both primary sources (mining) and secondary sources (recycling) will remain essential. Metals are inherently durable, with some metal-containing products and infrastructures lasting for decades or even centuries. In contrast, consumer goods like electronic devices and rechargeable batteries generally have shorter lifespans. These items contain a variety of valuable and critical metals [4].

Presently, the European Union has classified 34 resources, including cobalt, platinum group metals, and rare earth elements, as critical for the European industrial sector (Table 1) [5].

*Table 1 - Fifth list 2023 of Critical Raw Materials for the EU* [5].

| Critical Raw Materials | |
|---|---|
| Antimony | Light Rare Earth Elements |
| Arsenic | Lithium |
| Bauxite | Magnesium |
| Baryte | Manganese |
| Beryllium | Natural Graphite |
| Bismuth | Nickel* |
| Boron | Niobium |
| Cobalt | Phosphate rock |
| Coking Coal | Phosphorus |
| Copper* | Platinum Group Metals |
| Feldspar | Scandium |
| Fluorspar | Silicon metal |
| Gallium | Strontium |
| Germanium | Tantalum |
| Hafnium | Titanium metal |
| Helium | Tungsten |
| Heavy Rare Earth Elements | Vanadium |

*strategical raw materials

Unlike other raw materials such as fossil fuels or food, metals are not consumed; they maintain their inherent properties through recycling. This makes them perfect for repeated use without any loss in quality or functionality. As a result, metals are seen as a perpetually available resource, crucial for sustainable innovations in eco-friendly transportation, green energy, and digital communication systems (Figure 1) [4], [6].

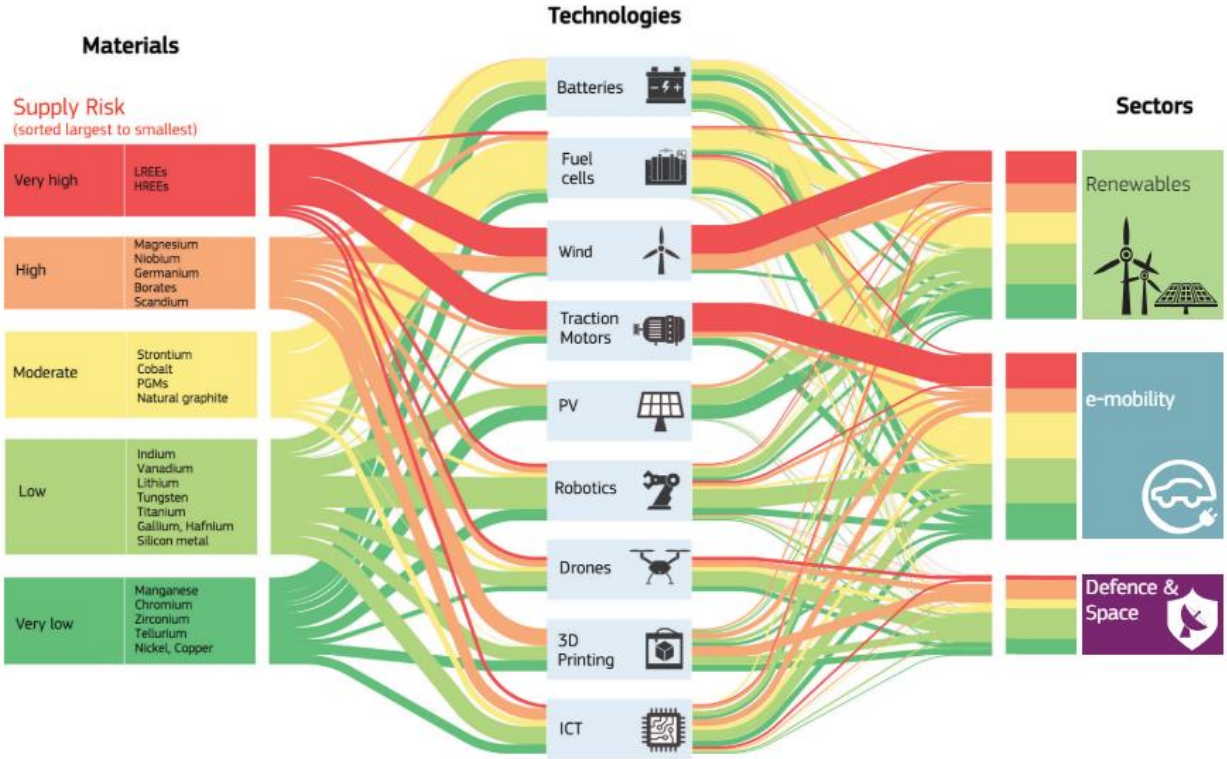



*Figure 1 - Critical raw materials technological applications and their current supply risks* [7].

Metal recycling offers an extremely efficient method for re-establishing valuable materials into the economy, addressing tactical challenges while reducing environmental effects and the energy intensity of material sourcing [4]. Establishing a circular economy entails efficiently recycling products at the end of their lifecycle, especially those with short lifespans like consumer electronics and rechargeable batteries, which contain valuable and critical metals. The main principle of circular economy is value recovery: all waste holds an essential value that can be extracted if managed properly. In the context of global environmental remedy, achieving sustainable, efficient, and cost-effective waste management has become increasingly vital [8].

The primary goal of a "circular economy" is to maintain the continuous flow of materials through successive product life cycles. This is achievable only when materials are reintroduced into production processes. Following the waste hierarchy, the emphasis should be on extending the use of products and materials as much as possible, by prioritizing waste prevention and recycling practices [4]. However, goods will inevitably reach the end of their

lifecycle, making it essential to provide access to recycling, prevent illegal waste exports, and employ the most advanced recycling technologies [4].

Waste electrical and electronic equipment (WEEE) is the world's fastest-growing waste stream, posing a considerable challenge due to its valuable components, diverse materials, and potential environmental hazards [9], [10]. Certain e-waste streams have higher concentrations of valuable metals (such as Au, Ag, Pd, In, Sb, Te, Ta, and rare earth elements) compared to their primary ores, making them a significant resource as secondary ores. Additionally, judicial pressure for the correct management and recycling of e-waste is increasing, with the EU WEEE Directive (2012/19/EU) recently raising collection and recycling targets.

Metal recycling techniques are based on hydro- and pyrometallurgy. While hydrometallurgy uses water to extract metals, pyrometallurgy relies on heat for the extraction and purification process [11]. While both hydro- and pyrometallurgy have their benefits, the industry generally favors hydrometallurgy over traditional pyrometallurgy. This preference arises from hydrometallurgy's effectiveness in recovering metals from diverse and challenging sources, including low-grade ores, complex metal ores, and secondary sources such as electronic waste [12]. However, conventional hydrometallurgical techniques for recycling e-waste are frequently inefficient and require aggressive acid or alkali digestion, complex multi-stage separation processes, large quantities of aqueous waste, and the use of flammable, volatile, and toxic solvents [13], [14]. Therefore, substantial efforts are required to develop more efficient, environmentally friendly, and sustainable alternatives, even though the economic and environmental benefits of metal recovery from e-waste are increasingly acknowledged.

## 2.2. Organic acids as alternative leaching reagents

Organic acids, as the name implies, are organic compounds with acidic characteristics. They are relatively weak acids that partially dissociate in water, and their strength is influenced by their functional groups, such as carboxyl (COOH) and sulfonic ($SO_3H$) [15]. The most prevalent organic acids feature a carboxyl group with the molecular formula (RCOOH). These acids are categorized based on their carbon chain structure, saturation, substitution, and functional groups. Many organic acids are naturally produced by microorganisms, making them environmentally friendly.

Due to their weaker nature, organic acids are anticipated to reduce or prevent the corrosion of costly equipment and minimize potential risks to operators. The low corrosion potential of organic acids on different metals and brass alloys is well-documented [16]. One study revealed that, among all tested acids — including inorganic acids (HCl, $HNO_3$, $H_2SO_4$)

and organic acids (acetic acid) — the organic acid exhibited the lowest corrosion potential. In addition to their low corrosion potential, organic acids do not emit toxic gases, unlike inorganic acids, and can function effectively at room temperature and pressure.

Several organic acids have been employed as leaching agents to recover metals from WEEE [17], [18], [19], [20]. Although organic acids are weaker than inorganic acids, numerous studies have demonstrated that the metal leaching efficiency of organic acids can be comparable to or even exceed that of commonly used inorganic acids [21].

The versatility, efficiency, and environmental sustainability of organic acids can facilitate various recycling strategies in closed-loop processes. These characteristics make organic acids highly suitable for sustainable recycling operations, supporting material reuse and minimizing environmental impact [20]. Furthermore, most organic acids are thermally stable, readily biodegradable, and do not persist in the environment. For instance, strong organic acids like oxalic acid can completely degrade in water within 5 days [22]. In contrast, inorganic acids are non-biodegradable, harmful to the environment, and have been linked to carcinogenicity [23]. Additionally, many organic acids are highly selective. [20]

## 2.3. Acidic aqueous two-phase systems

Aqueous two-phase systems (ATPS) are formed when two water soluble solutes, such as two polymers, two salts or a polymer and a salt, become incompatible in aqueous solution at concentrations above specific critical thresholds. This incompatibility causes the solution to separate into two distinct aqueous phases, each enriched in one of the solutes [24]. For example, when two polymers are mixed, they form large aggregates, and the two polymers tend to separate into different phases due to steric exclusion. A similar exclusion phenomenon can be observed between a polymer and a salt. In this case, the salt captures a significant amount of the water present in the system, leading to phase separation [25].

ATPS are characterized by a solubility curve that distinguishes the two-phase region from the single-phase region. The phase diagram outlines the feasible working area for a specific two-phase system and serves as a unique "fingerprint" for that system under defined conditions, such as pH, temperature, and salt or polymer concentration. The solubility curve specifies the exact compositions of the top and bottom phases in an ATPS. Compositions below the solubility curve are homogeneous, while two distinct phases are formed by compositions above the curve. Traditionally, solubility curves are determined by using the cloud point titration method [26].

Conventional metal liquid-liquid extraction systems often depend on non-ecofriendly volatile organic diluents to reduce the viscosity of extractants. Ionic liquids (ILs) were identified as a potential solution to this issue [27]. ILs are organic salts that present melting

temperatures below 373 K. They consist of an organic cation with a variable alkyl chain length and either an organic or inorganic anion. These liquids present tunable properties, namely polarity, hydrophobicity, and hydrogen-bonding capabilities [28]. The application of ILs in the formation of ATPS when mixed with polymers and salts was deeply studied in the past years and remarkable results were obtained in the extraction and separation of several kinds of molecules [26], [29]. However, the application of ATPS to metal extraction was always limited by their incompatibility with the low pH environment required to keep metals stable in aqueous solution [30].

Thus, in the search for improved metal extraction systems, it was developed a new type of acid-induced ATPS, known as acidic ATPS (AcATPS) [31]. Several studies have demonstrated that AcATPS can effectively extract and separate transition metals and rare earth elements [31], [32], [33]. In these new systems, the inorganic salt typically used in the formation of ATPS is replaced by an acid. This acid not only acts as a salting-out agent but also facilitates the leaching and stabilization of metals simultaneously. Typically, the phase with the highest acid mass fraction percentage is referred to as the acid-rich phase, while the phase with the highest IL mass fraction percentage is known as the IL-rich phase. Like conventional ATPS, AcATPS can exhibit thermoresponsive behavior, specifically a lower critical solution temperature (LCST) [34], [35]. This new type of systems closes the gap between ATPS and metallic ion extraction from acidic phases. Such versatile systems could facilitate the integration of leaching and liquid-liquid extraction unit operations on metals recycling processes [2].

### 2.3.1. Effect of ionic liquid and acid in acidic aqueous two-phase systems

Due to the complex mechanisms behind the formation of these systems, only a reduced number of ILs can be used to induce the formation of AcATPS. Schaeffer et al. [36] demonstrated that only ILs constituted by quaternary ammonium ($[N_{nnnn}]^+$) or quaternary phosphonium ($[P_{nnnn}]^+$) cations with $n \geq 4$ are able to induce phase separation in the presence of acids. Authors demonstrated that this is related to the apparent charge at the surface of IL cation, which needs to be neutral[36]. Thus, the IL tributyltetradecylphosphonium chloride ($[P_{44414}]Cl$) is the most commonly used in the formation of AcATPS.

Most of the reported works on AcATPS are related to the use of inorganic acids: HCl, $H_2SO_4$, and $HNO_3$. The impact of the acid on the formation of these systems was also evaluated and two main factors need to be considered: (i) the degree of dissociation of the acid, and (ii) the occurrence of anion exchange between the acid and IL anions [36]. For example, phosphoric acid is not able to induce the formation of AcATPS. This is related to the fact that this acid does not fully dissociate in aqueous solution. Furthermore, when nitric acid is used there is the formation of a hydrophobic IL due to anion exchange.

Despite the high interest in the use of organic acids as leaching agents and consequently, as phase-forming compounds of liquid-liquid extraction systems, only a single work was reported with the use of acetic acid for the formation of AcATPS in the presence of $[P_{44414}]Cl$.

### 2.3.2. Temperature impact

As previously referred, $[P_{44414}]Cl$ has been used on AcATPS, demonstrating compatibility with both inorganic and organic acids [2], [37]. The solubility of IL-based systems that respond to temperature changes is marked by an upper or lower critical solution temperature (UCST or LCST). These transitions occur due to predominant entropic effects for LCST and enthalpic effects for UCST, arising from the interactions between ILs and water. Key interactions involve hydrogen bonding and strong polar interactions [38], [39].

A previous study showed that the phase separation of an AcATPS composed of $[P_{44414}]Cl$ is enhanced by increasing temperature. This means that less acid is required to induce an ATPS at higher temperatures, demonstrating a LCST type behavior [35]. In fact, certain hydrophilic quaternary salts, such as $[P_{4444}]Cl$ and its surfactant derivative $[P_{44414}]Cl$, exhibit a pronounced LCST behavior when mixed with water [35], [40], [41], [42], [43]. Moreover, the LCST transition in AcATPS is dynamic and non-linear, affected by factors such as the IL concentration and the phase behavior of the IL in solution at specific acid-to-IL ratios, which can be in micellar or bicontinuous regimes [35]. In concentrated $[P_{44414}]Cl$ solutions, the system transitions from an aqueous IL solution to a hydrated IL [44]. These 'solvent in salts' systems exhibit significantly different dynamics compared to their aqueous counterparts. This suggests that as the IL content increases, the impact of temperature on phase separation may change depending on the “rigidity” of the $[P_{44414}]Cl$ self-organization [35].

### 2.3.3. Metal partition

Metal ions extracted by unfunctionalized quaternary phosphonium or ammonium ILs form anionic complexes [45]. In chloride-rich systems, the distribution ratio of each metal is governed by their propensity to form chloro-complexes, along with the stability and affinity of these complexes for the IL-rich [31], [46]. Metal complexes with lower charge densities are more likely to partition into the IL-rich phase. This partition is affected by the presence of anions, whether from the IL or the acid, which can create anionic complexes stabilized in the IL-rich phase. Additionally, the co-extraction of acid can influence metal distribution by hindering the extraction of metal complexes into the IL-rich phase [47]. The adaptability of AcATPS positions them as a capable alternative to conventional liquid-liquid extraction systems, with ILs acting both as phase-forming agents and as extractants [47].

# 3. Materials and Methods

## 3.1. Materials and Instrumentation

### 3.1.1. Materials

The ATPS and AcATPS studied in this work were established by preparing ternary mixtures composed of ILs, organic acids and water. The ILs tetrabutylphosphonium chloride ([$P_{4444}$]Cl, 95.0 m% pure), and tributyltetradecylphosphonium chloride ([$P_{44414}$]Cl, 95.0 m% pure) were purchased from Iolitec (Heilbronn, Germany) and used as received. Their chemical structures are presented in Figure 2. Citric acid (≥99%) and propionic acid (≥99%) were purchased from Merck (Darmstadt, Germany). Acetic acid (99.7%), potassium citrate monohydrate (≥99%), lactic acid (88%-92%) and butyric acid (≥99%) were purchased from Sigma-Aldrich (St. Louis, MO, USA). Sodium acetate (99%), sodium formate (≥99%), and copper chloride (≥98%) were purchased from AnalaR NORMAPUR® ACS (Vienna, Austria). Formic acid (99%) was purchased from Carlo Erba (Emmendingen, Germany). All chemicals were used as received. Distilled water was used. The chemical structure and properties of the studied carboxylic acids are presented in Table 2.

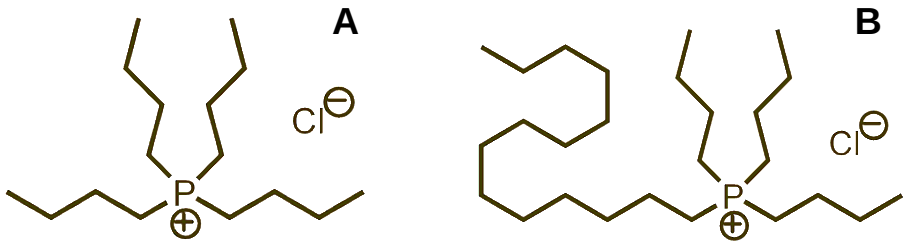
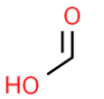
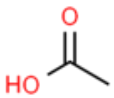
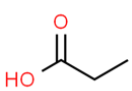
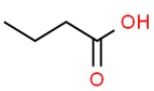
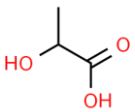
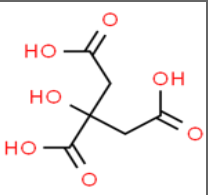



*Figure 2 - Chemical structure of the IL evaluated in this work: (A) [$P_{4444}$]Cl; (B) [$P_{44414}$]Cl.*

*Table 2 - Carboxylic acids used in this work and their properties.*

| Acid | Formic | Acetic | Propionic | Butyric | Lactic | Citric |
|---|---|---|---|---|---|---|
| Molecular Formula | $CH_2O_2$ | $C_2H_4O_2$ | $C_3H_6O_2$ | $C_4H_8O_2$ | $C_3H_6O_3$ | $C_6H_8O_7$ |
| Structure |  |  |  |  |  |  |
| Alkyl group | 0 | 1 | 2 | 3 | 1 | 0 |
| Carboxyl group | 1 | 1 | 1 | 1 | 1 | 3 |
| p$K_a$[48] | 4.27 | 4.54 | 4.75 | 4.91 | 3.78 | 3.0 3.2 |
| log($K_{ow}$) at pH 1.7[48] | -0.27 | -0.22 | 0.48 | 0.92 | -0.48 | -1.33 |

## 3.2. Liquid-liquid equilibria

Ternary systems composed of IL + acid + water and IL + salt + water, as well as quaternary systems composed of IL + acid + salt + water, were evaluated in this work. The phase diagrams were obtained using the cloud point titration method [49], [50] in a temperature-controlled cell at (298±1) K and atmospheric pressure. For the ternary systems, aqueous solutions of the ILs at concentrations ranging between 80 and 60 m% and aqueous solutions of the different organic acids or salts at concentrations close to their water solubility were prepared. Drops of the aqueous solutions of organic acids or salts were added to the IL solution until the solution turned cloudy, indicating the formation of a biphasic system. Distilled water was then added dropwise until the solution became clear again (monophasic region). This process was repeated to obtain a series of cloud points, which correspond to the solubility curve, delineating the boundary between the monophasic and biphasic states. The phase diagrams for the quaternary systems were determined by the same procedure, however, the salt or the acid was added at a fixed concentration (5 m%) at all the solutions used (including the water). The ternary and quaternary system compositions were determined by the quantification within an uncertainty of $10^{-4}$ g.

### 3.2.1. Determination of tie-lines and tie-line length

Literature reviews indicate that no previous efforts have been made to create an equation that can simultaneously correlate the solubility curves for systems with different solvents. While various empirical equations have been utilized to correlate experimental binodal data, they were not designed for multiple systems [51], [52], [53], [54], [55], [56].

Rogers and co-workers [57] applied the empirical model, originally proposed by Merchuk et al. [56] for polymer-based systems, to describe the experimental curves of IL-based ATPS. They successfully fitted the solubility curves of ternary systems composed of ILs, salts, and water to a three-parameter equation. In this model, [IL] and [salt] represent the mass fraction percentages (m%) of the IL and salt, respectively, while A, B, and C are fitting parameters determined by least squares regression.

$$[IL] = A \exp\left(B[salt]^{0.5} - C[salt]^3\right) \quad (1)$$

Merchuk et al. [56] initially suggested a gravimetric technique to ascertain the tie-lines (TLs) in polymer-based systems, involving the use of equation (1) combined with a mass balance relationship. The lever-arm rule is utilized to establish the compositions of the top and bottom phases as well as the overall system compositions. Rogers and colleagues [57] effectively implemented this method for IL-based ATPS. Each TL is calculated based on solving the following system of four unknown constants,

$$[IL]_{IL} = A \exp\left[\left(B \times [salt]_{IL}^{0.5}\right) - \left(C \times [salt]_{IL}^{3}\right)\right] \quad (2)$$

$$[IL]_{salt} = A \exp\left[(B \times [salt]_{salt}^{0.5}) - (C \times [salt]_{salt}^{3})\right] \quad (3)$$

$$[IL]_{IL} = \frac{[IL]_M}{\propto} - \frac{1-\propto}{\propto} \times [IL]_{salt} \quad (4)$$

$$[salt]_{IL} = \frac{[salt]_M}{\propto} - \frac{1-\propto}{\propto} \times [salt]_{salt} \quad (5)$$

In equations (2) – (5), the subscripts "IL", "salt", and "M", designate the IL-rich phase, the salt-rich phase, and the mixture, respectively; [*IL*] and [*salt*] represent the mass fraction percentage (m%) of the salt and of the IL, respectively; $\alpha$ is the ratio between the mass of the IL-rich phase and the total mass of the mixture. The tie-line length (TLL) was calculated by the following equation:

$$TLL = \sqrt{([salt]_{IL} - [salt]_{salt})^2 + ([IL]_{IL} - [IL]_{salt})^2} \quad (6)$$

The pH (±0.02) of the phases that composed the system $[P_{44414}]Cl + C_6H_5K_3O_7 + H_2O$ was measured at (298 ± 1) K using a Titroline 6000 pH meter with a precision of 0.1%.

### 3.2.2. In-phase water and $Cl^-$ anion quantification

To better understand the mechanisms that rule the formation of ATPS composed of organic acids, the water content and $Cl^-$ anion concentration on the phases that composed the following systems was determined: $[P_{44414}]Cl$ + formic acid + water and $[P_{44414}]Cl$ + butyric acid + water. The water content of the top and bottom phases was determined using coulometric Karl Fisher titration with a Titroline 7500 KF Trace (SI Analytics Karl Fischer). The chloride anion content was determined using a chloride ion selective electrode.

### 3.2.3. Determination of aggregate size

The size of aggregates formed in an aqueous solution of $[P_{44414}]Cl$ in the presence of the citric acid was measured by dynamic light scattering (DLS) using a Malvern Zetasizer Nano-ZS.

### 3.2.4. Cu partition and quantification

The extraction efficiency of copper on the quaternary system composed of 30 m% $[P_{44414}]Cl$ + 12 m% $C_6H_8O_7$ + 5 m% $K_3C_6H_5O_7$ + 53 m% $H_2O$ was determined. The quaternary mixture was gravimetrically prepared, and water was substituted by a copper aqueous solution at 0.2 M. The top and bottom phases were separated and analyzed by UV-visible spectroscopy, using a Varioskan Flash Multimode Microplate (Thermo Scientific) at a wavelength of 817 nm and using a calibration curve previously established.

# 4. Results and Discussion

To identify potential mixtures capable of inducing liquid phase separation, aqueous solutions of chloride-based ILs ([$P_{4444}$]Cl and [$P_{44414}$]Cl) and six organic acids (formic, acetic, propionic, butyric, lactic and citric acids) were screened for the existence of a biphasic regime. Table 3 summarizes the tested mixtures and the obtained results. From the initial screening, only mixtures of [$P_{44414}$]Cl with the acids studied were able to induce the formation of a biphasic system, with all others remaining monophasic under the explored conditions. It is important to highlight that [$P_{44414}$]Cl-acetic acid system was previously reported [2] and is presented in this work for comparison with the remaining carboxylic acids. Vargas et al.[2] also reported the inability of acetic acid to induce the formation of a two-phase system in the presence of [$P_{4444}$]Cl.

*Table 3 – Summary of the ternary mixtures evaluated and their ability to induce (✓) or not (X) the formation of a biphasic system.*

| Acid/IL | [$P_{4444}$]Cl | [$P_{44414}$]Cl |
|---|---|---|
| Formic | ✗ | ✓ |
| Acetic [2] | ✗ | ✓ |
| Propionic | - | ✓ |
| Butyric | - | ✓ |
| Lactic | - | ✓ |
| Citric | ✗ | ✓ |

As mentioned before, the IL hydrophobic character can be influenced by the anionic or cationic alkyl chain length. Knowing that [$P_{4444}$]Cl and [$P_{44414}$]Cl have the same inorganic anion and only differ in the length of one of the alkyl chains (see Figure 2), it seems clear that this is the main reason behind the very distinct results. In fact, [$P_{44414}$]Cl presents a surfactant behavior. It was previously demonstrated that this is a very important characteristic for its ability to induce the formation of acid ATPS in the presence of inorganic acids [36].

## 4.1. The effect of carboxylic acids

The solubility curves obtained with the ternary mixtures composed of [$P_{44414}$]Cl + carboxylic acids + water at 298 K are presented in Figure 3. The experimental data of each solubility curve can be found in the Appendix A. For all AcATPS examined, the IL-rich phase is at the top, and the acid-rich phase is at the bottom. The results are expressed in molality

units to better understand the influence of carboxylic acid on the phase diagram behavior, avoiding discrepancies due to different molecular mass. The biphasic region lies above the curve, while the monophasic region is below. Therefore, a larger biphasic region indicates a greater ability of the acid to induce phase separation in the presence of $[P_{44414}]Cl$. Again, it is important to highlight that experimental data of acetic-acid-based system was previously reported [2] and is here presented for comparison reasons.

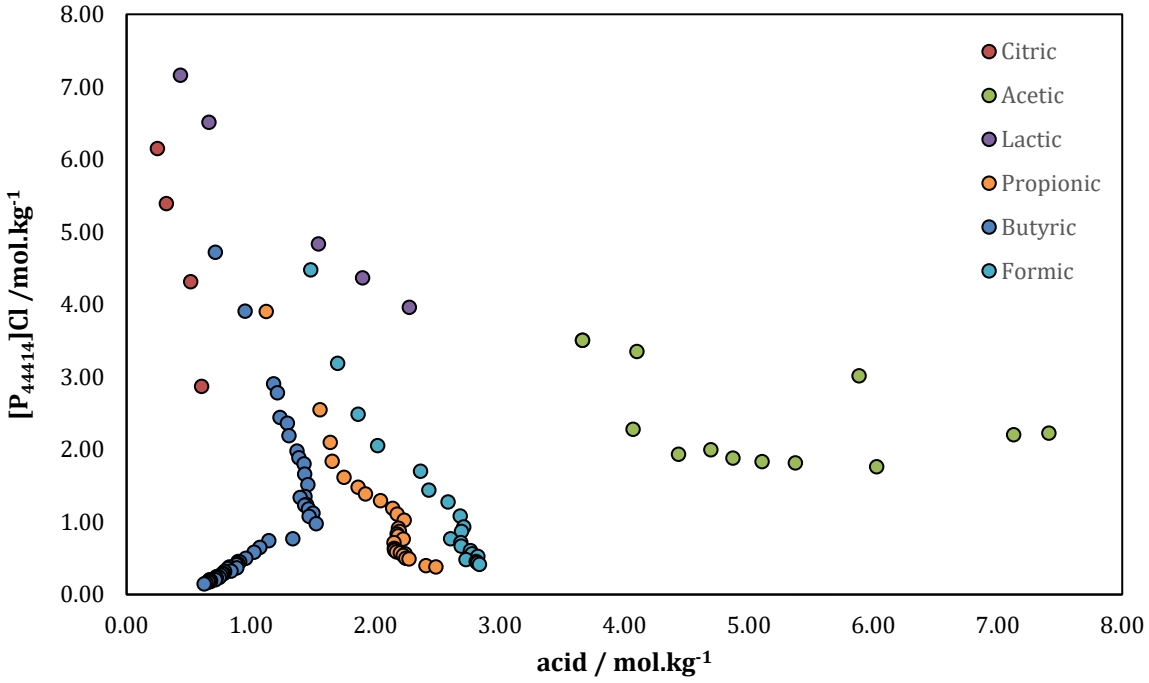



*Figure 3 - Evaluation of the carboxylic acid nature impact in the ternary phase diagrams composed of $[P_{44414}]Cl$ + organic acid + water. Experimental data for the acetic acid binodal curve were previously reported and are used here for comparison purposes [2].*

The results presented in Figure 3 show that the solubility curves obtained by mixing the different carboxylic acids with the IL $[P_{44414}]Cl$ present unexpected behaviors. The ability of carboxylic acids to induce the formation of AcATPS in the presence of $[P_{44414}]Cl$ presents the following trend: citric > butyric > propionic > formic > lactic > acetic acid. Acetic acid presents a type 0 phase diagram which was discussed elsewhere [2]. No other acid presents a similar behavior.

The acid impact on the formation of AcATPS is typically ruled by two main mechanisms: (i) the degree of dissociation and (ii) the possible occurrence of anion exchange [36], [37]. At the current experimental conditions, all carboxylic acids are mainly in their protonated form (see Table 2), which reduces the possibility of ion exchange. Furthermore, when looking only for the mono-carboxylic acids with increased alkyl chains (formic, acetic, propionic, and butyric acid) it is possible to observe a tendency to increase the biphasic region with the increase of the alkyl chain, except for formic acid. This suggests the presence

of dispersive interactions that may occur between the IL and the aliphatic segments of carboxylic acids, inducing easier phase separation in the presence of long alkyl chains. Furthermore, the solubility curve of butyric acid exhibits unusual behavior; beyond a certain concentration, the solubility curve reverses, indicating an increase in immiscibility. Similarly, the solubility curves of propionic and formic acids show some discontinuities, although these are less pronounced compared to those of butyric acid.

Concerning lactic and citric acids, probably their behaviors are explained by different mechanisms than those previously discussed. Despite having a single carboxyl group, lactic acid includes an additional hydroxyl group which results in higher hydration and consequently a lower ability to induce the phase separation when compared, for example, with propionic acid. On the other hand, poly-carboxylic citric acid presents a larger biphasic region. This behavior seems to be more in line with conventional ATPS, in which the phase separation is mainly ruled by the ability of the solutes to form hydration complexes [26].

To better understand the mechanisms that rule the formation of these systems, two mixture points for both butyric- and formic-acid-based systems were prepared, and the pH, the water content, and the $Cl^-$ anion concentration in both phases were determined. The obtained results are presented in Table 4. Concerning the water distribution between the coexisting phases, the obtained results are in line with what is commonly observed for acidic ATPS, with the acid-rich phase richer in water than the IL-rich phase. However, it is quite remarkable that the acid-rich phases of butyric-acid-based systems present a water concentration > 97 m% This result suggests that the acid is mainly present in the IL-rich phase which supports the theory that dispersive interactions between the IL and the acid occur. Furthermore, this also explains the behavior of the solubility curve of butyric acid.

*Table 4 – pH, water content, and chloride anion concentration on both IL- and acid-rich phases of systems composed of $[P_{44414}]Cl$ + formic or butyric acid + $H_2O$.*

| Acid | IL (m%) | Acid (m%) | Phase | pH | $[H_2O]$ (m%) | $[Cl^-]$ (m%) |
|---|---|---|---|---|---|---|
| Formic | 25 | 15 | Top | 1.46 | 13.59 | - |
| | | | Bottom | 0.67 | 87.42 | 7.69 |
| | 32 | 15 | Top | 1.39 | 13.55 | - |
| | | | Bottom | 0.61 | 89.23 | 2.57 |
| Butyric | 15 | 10 | Top | 2.99 | 12.50 | - |
| | | | Bottom | 1.53 | 99.11 | 0.45 |
| | 15 | 15 | Top | 2.77 | 11.73 | - |
| | | | Bottom | 1.32 | 97.95 | 0.37 |

Unfortunately, it was not possible to quantify the chloride anion in the IL-rich phase due to its very low water solubility. Nevertheless, the results obtained for the bottom phases show a much higher concentration of this anion in formic acid systems than in butyric acid systems. To complete this data, it will be important to quantify the amount of $[P_{44414}]^+$ cation in both phases and evaluate if ion exchange is also occurring in these systems.

## 4.2. Acid vs salt-based aqueous two-phase systems

Figure 4 presents the results obtained for the systems composed of potassium citrate, sodium formate, or sodium acetate with $[P_{44414}]Cl$ and their comparison with the respective acid-based systems. Through these results, it is possible to infer the impact of the acid proton in the formation of the two-phase system. It is evident that proton impact on acetic and formic acids-based systems (Fig. 4B and 4C) is more pronounced than in citric acid (Fig. 4A), which seems to support the theory that different mechanisms are present in these systems. Furthermore, when the impact of salt is evaluated (see Fig. 4D) it is possible to observe that the solubility curves almost overlap suggesting that salt nature impact is much lower than in the case of acids. Still, it is possible to distinguish the following trend: citrate > formate > acetate salt. This trend agrees with the trend observed for carboxylic acids.

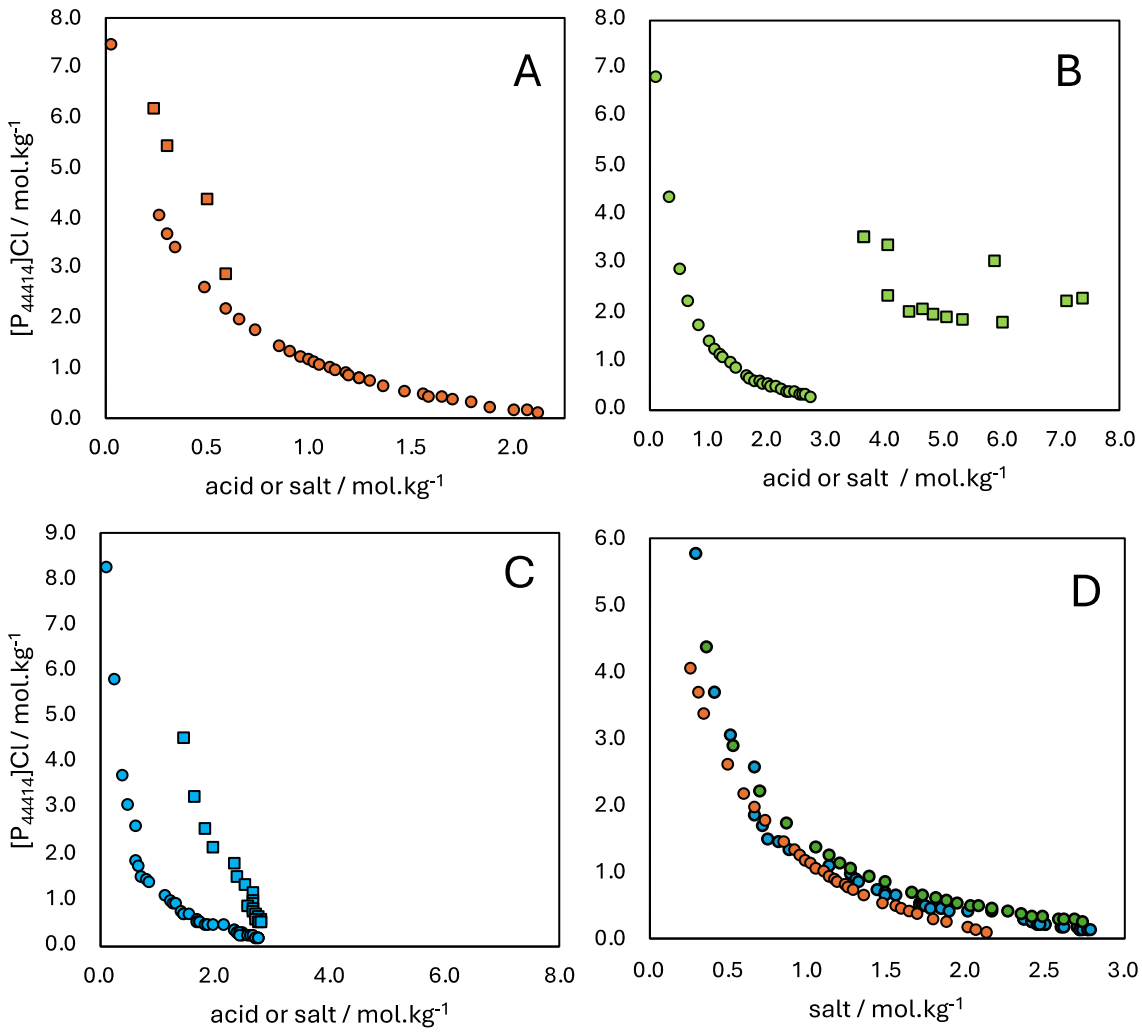



*Figure 4 - Comparison between acid- and salt-based ATPS composed of [$P_{44414}$]Cl and (A) potassium citrate (●) or citric acid (■); (B) sodium acetate (●) or acetic acid (■); (C) sodium formate (●) or formic acid (■). (D) The influence of salt on ATPS composed of [$P_{44414}$]Cl.*

## 4.3. Temperature effect

It was previously reported that AcATPS composed of [$P_{44414}$]Cl presents a LCST behavior allowing improvement in the phase separation by the increase of temperature [2]. The temperature effect on the citric-acid-based system was evaluated and the obtained results are presented in Figure 5. From Figure 5, it is possible to see that the temperature affects the biphasic system, which became closer to the axis; however, this effect is small, and it didn't allow for a complete solubility curve. Schaeffer et al. [35] reported that solubility curves of [$P_{44414}$]Cl + HCl + $H_2O$ as a function of temperature present two main domains: (i) a highly temperature-dependent domain for [$P_{44414}$]Cl concentration below 50 m% and (ii) a lesser temperature-dependent one for [$P_{44414}$]Cl concentration above 50 m%. Despite this behavior having been only reported for HCl-based systems, this can help to comprehend why the temperature effect is not significant for citric-acid-based systems. In fact, it was not

possible to obtain experimental data below 55 m% of IL at any of the temperatures evaluated.

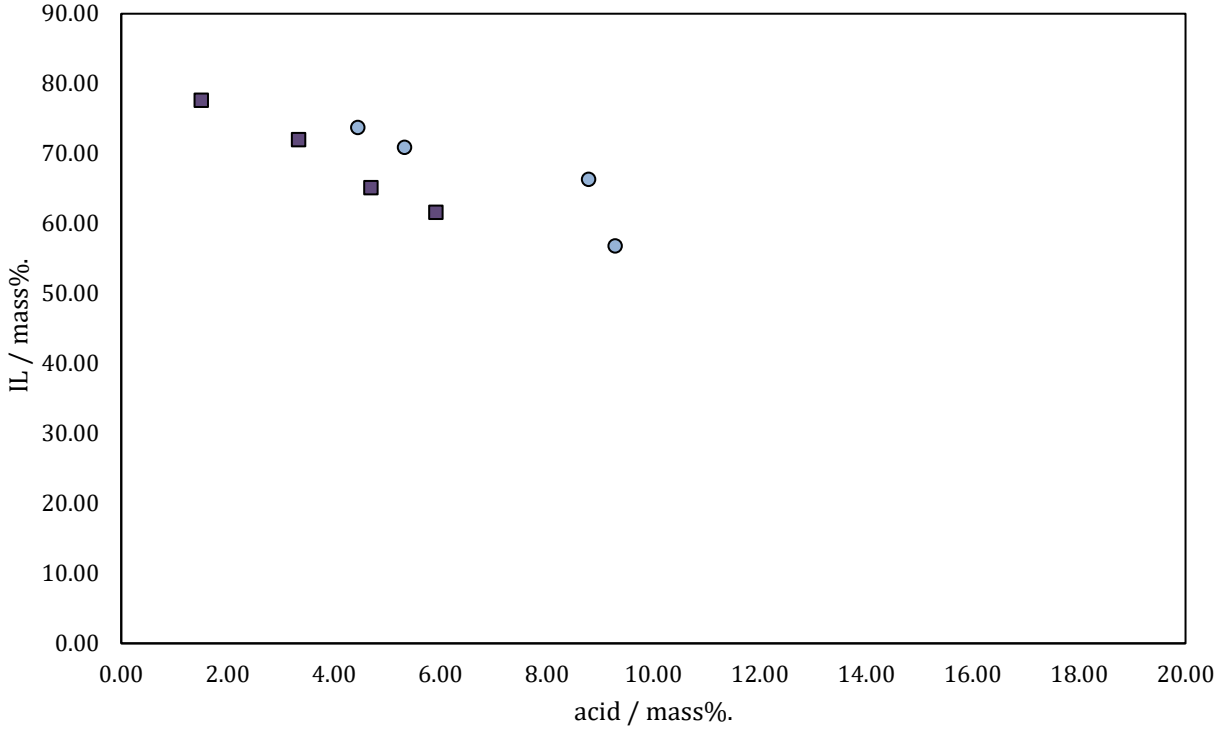



*Figure 5 - The temperature effect on citric-acid-based ATPS: 298 K (●); 323 K (■).*

## 4.4. Merchuk equation and tie-lines determination

Among all the solubility curves determined in this work, only the solubility curves of salt-based systems can be fitted by the correlation proposed by Merchuk et al. [56] (Eq. 1), since acid-based one presents discontinuities that are not possible to describe with this equation. The values obtained for the regression parameters are presented in Table 5.

*Table 5 - A, B, and C parameters and correlation coefficients, $R^2$, obtained for ATPS composed of $[P_{44414}]Cl$ + salt + $H_2O$ at 298 K.*

| Salt | A | B | $10^5$ (C) | $R^2$ |
|---|---|---|---|---|
| Citrate | 140.92 | -0.53 | 1.56 | 0.9794 |
| Acetate | 116.80 | -0.36 | 18.3 | 0.9305 |
| Formate | 142.92 | -0.52 | 31.9 | 0.9855 |

Two experimental TLs were determined for the system composed of $[P_{44414}]Cl$ + $K_3C_6H_5O_7$ + $H_2O$, along with their respective TLL. The pH of coexisting phases was also measured. The obtained results are presented in Table 6 and Figure 6.

*Table 6 - Mass fraction percentage (m%) for the coexisting phases of the systems $[P_{44414}]Cl + K_3C_6H_5O_7 + H_2O$, and respective values of TLL, and pH values of each phase.*

| $[IL]_{IL}$ | $[salt]_{IL}$ | $pH_{IL}$ | $[IL]_M$ | $[salt]_M$ | $[IL]_{salt}$ | $[salt]_{salt}$ | $pH_{salt}$ | TLL |
|---|---|---|---|---|---|---|---|---|
| 9,92 | 22,28 | 8,55 | 70,75 | 24,83 | 60,83 | 2,55 | 7,99 | 54,59 |
| 13,26 | 18,55 | 8,32 | 63,03 | 22,46 | 49,77 | 3,91 | 7,96 | 39,34 |

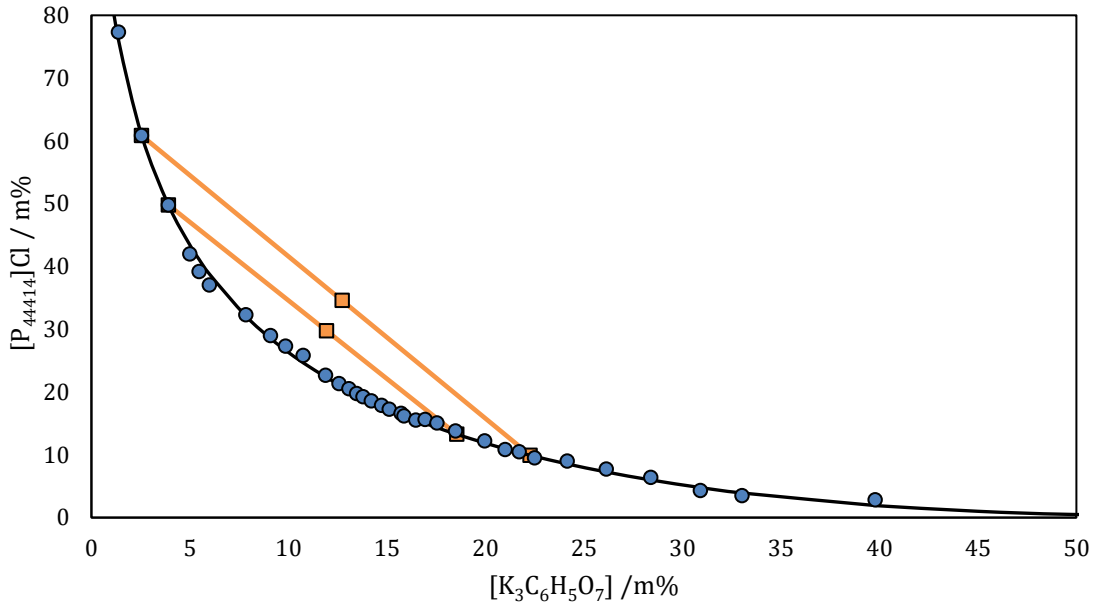



*Figure 6 - Phase diagram for the ternary system composed of $[P_{44414}]Cl + K_3C_6H_5O_7 + H_2O$, at 298 K and atmospheric pressure: solubility curve data (●), TL data (■), adjusted solubility data through Eq. (1) (–).*

## 4.5. Phase diagrams of quaternary mixtures

Aiming to find a solution for the use of organic acids as phase-forming compounds, the phase diagrams of quaternary mixtures composed of $[P_{44414}]Cl + K_3C_6H_5O_7 + C_6H_8O_7 + H_2O$ were evaluated. Two new solubility curves were determined, one with a fixed amount of 5 m% of potassium citrate, and the other with a fixed amount of 5 m% of citric acid. The obtained results and their comparison with the solubility curves of the ternary systems constituted by the IL/salt and IL/acid are presented in Figure 7.

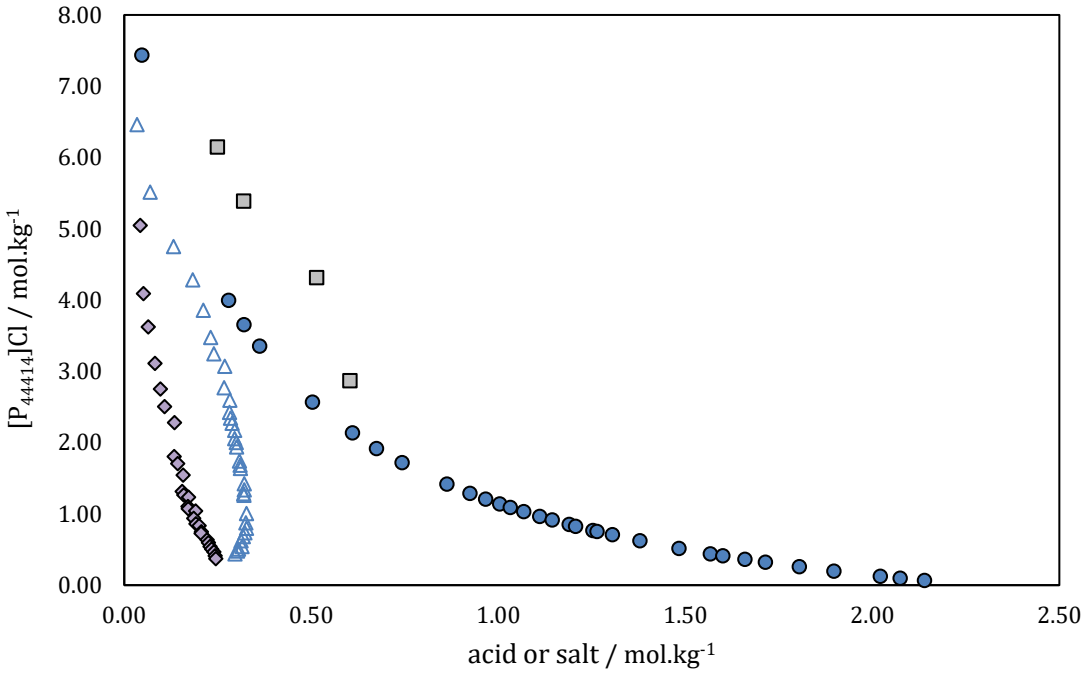



*Figure 7 - Liquid-liquid equilibria of quaternary and ternary systems composed of $[P_{44414}]Cl$, $K_3C_6H_5O_7$, $C_6H_8O_7$, and $H_2O$: $[P_{44414}]Cl + K_3C_6H_5O_7 + H_2O$ (●); $[P_{44414}]Cl + K_3C_6H_5O_7 + 5$ m% $C_6H_8O_7 + H_2O$ (◆); $[P_{44414}]Cl + 5$ m% $K_3C_6H_5O_7 + C_6H_8O_7 + H_2O$ (▲); $[P_{44414}]Cl + C_6H_8O_7 + H_2O$ (■).*

Quaternary systems composed of acids and salts were previously reported for the selective separation of metals. The addition of salt to the acidic system allows for tuning its properties and improves metal separation [58]. However, and against what we were expecting, the addition of 5 m% of potassium citrate to the citric-acid-based system induced a similar effect to that observed for the butyric acid solubility curve (Fig. 3 and 7). On the other hand, if 5 m% of acid is added to the system composed of the salt, the biphasic region drastically increases.

To better understand the non-conventional behavior of the solubility curve of the quaternary systems composed of 5 m% of salt, the size of the aggregates present in the solution at different concentrations of acid and IL was determined. The obtained results are presented in Figure 8.

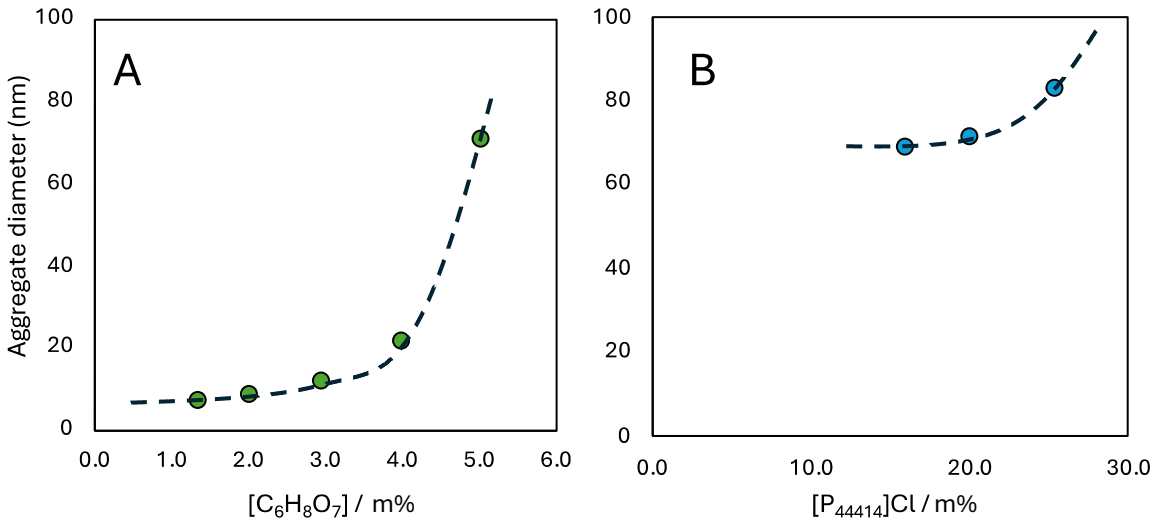



*Figure 8 - The effect of (A) citric acid (at a fixed concentration of 20 m% of IL) and (B) $[P_{44414}]Cl$ (at a fixed concentration of 5 m% of acid) concentration on average aggregate diameter present in $[P_{44414}]Cl + C_6H_8O_7$ + 5 m% $K_3C_6H_5O_7 + H_2O$.*

Through the results presented in Figure 8, it is possible to see that the increase of acid concentration has a much higher impact on the size of the aggregates induced by the $[P_{44414}]Cl$ in aqueous solution than the IL. Again, these results seem to be in line with the results obtained and reported here for the other carboxylic acids. However, more studies need to be carried out to understand if these same effects are observed in the ternary systems.

Despite the phase separation behavior of citrate-based quaternary systems is not completely understood, it was carried out an experiment to evaluate the potential use of this system for Cu extraction. A mixture composed of 30 m% $[P_{44414}]Cl$ + 12 m% $C_6H_8O_7$ + 5 m% $K_3C_6H_5O_7$ + 53 m% $H_2O$ was used for the partition of Cu. Only 14.3 % of Cu was extracted to the IL-rich phase. Metals extraction on AcATPS occurs by the formation of complexes with the ions present in the solution, namely with chloride [47]. However, the UV-vis spectra obtained for this metal (Figure 9) on both system phases, and the characteristic blue color present in the system, show that Cu is in the form of $[Cu(H_2O)_6]^{2+}$ complex, suggesting that the concentration of $Cl^-$ present in the system is not enough to induce the formation of copper-chloride complexes $[CuCl_4]^{2-}$ that are more favorable to the partition of this metal to the IL-rich phase [47]. These preliminary results suggest that more work needs to be carried out on the design of these systems to allow their application in metal extraction and separation.

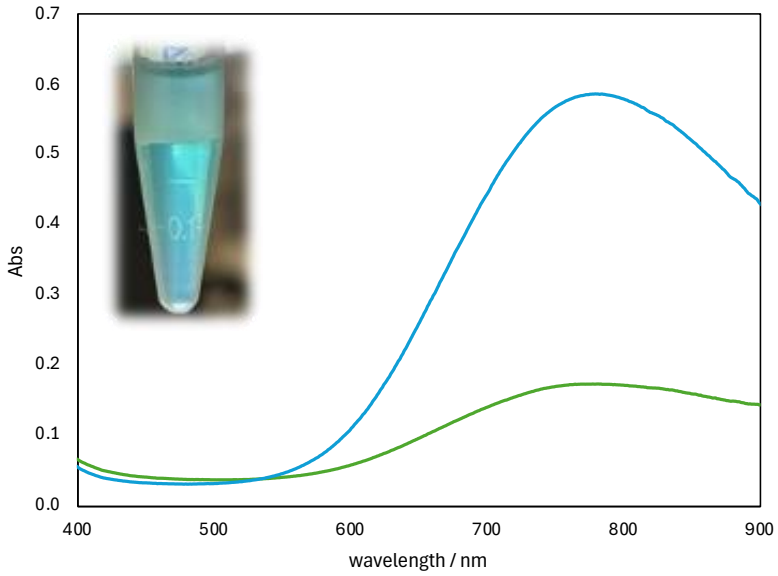



*Figure 9 -The UV-vis spectra of Cu on top (blue) and bottom (green) phases of the system $[P_{44414}]Cl + C_6H_8O_7 + K_3C_6H_5O_7 + H_2O$.*

# 5. Conclusion

The present study brings new insights on the phase behavior of ternary mixtures containing the hydrophilic IL tributyltetradecylphosphonium chloride, $[P_{44414}]Cl$, and different organic acids. The obtained phase diagrams revealed key factors that influence the two liquid phases separation in these systems.

In AcATPS, the choice of the IL is crucial for the formation and performance of the system. Despite being hydrophilic, $[P_{44414}]Cl$ has a long cationic alkyl chain, which confers hydrophobic characteristics to the IL within these systems, leading to surfactant-like behavior. Regarding the effect of carboxylic acids such as formic, acetic, propionic, and butyric acid, there is a noticeable trend: the biphasic region expands with the lengthening of the alkyl chain. Furthermore, the solubility curve of butyric acid exhibits unusual behavior showing an increase in immiscibility. Lactic acid, although a carboxylic acid, contains a hydroxyl group, which leads to a higher hydration and a lower ability to induce the phase separation. In contrast, poly-carboxylic citric acid exhibits a larger biphasic region, like conventional ATPS. This allows us to assess the influence of additional functional groups on phase behavior in AcATPS. Against to what was expected temperature influence on citric-acid-based system was very low. Finally, the development of hybrid systems composed of citric acid and potassium citrate was evaluated. However, the system's behavior proved to be complex.

The potential use of a citrate-based quaternary system for copper (Cu) extraction was evaluated. The system used, resulted in only 14.3% of Cu being partitioned into the IL-rich phase. These findings highlight the need for further research and optimization in the design of citrate-based quaternary systems for metal extraction and separation.

These preliminary results underscore the complexity of organic acid-based ATPS and the necessity for detailed studies to develop efficient systems for metal recovery and their integration on recycling processes.

# 6. Assessment of the work done

## 6.1. Objectives Achieved

This research has proposed a potential solution to metal separation by the application of organic acids instead of the more aggressive and toxic commonly used inorganic acids. The objective was to evaluate their potential as phase-forming compounds in AcATPS to reach the selective separation of critical and strategic metals. The study has successfully met its primary objective of characterizing organic-acid-based ATPS to later assess their viability in metal separation.

Following the characterization of AcATPS using organic acids, these systems were applied in metal separation experiments. Although the systems demonstrated some distribution of metals between the phases, the partition wasn't enough to proceed to metal extraction. Specifically, the partition of copper resulted in only 14.3% of Cu being separated into the IL-rich phase. These results indicate that further investigation and optimization are necessary to improve the efficiency of metal separation using AcATPS.

## 6.2. Contribution to the Sustainable Development Goals

This work contributes significantly to several Sustainable Development Goals (SDGs) by promoting sustainable industrial practices and environmental protection – Table 7.

*Table 7 - Contribution to the SDGs - SDGs applied in this report* [59].

| SDGs | Goal | Contribution | Performance Indicators and Metrics |
|---|---|---|---|
| 8. Decent Work and Economic Growth | 8.4 Improve resource efficiency | Enhanced resource efficiency in metal recovery processes | Amount of metals recovered, cost savings from recycling vs. mining |
| 9. Industry, Innovation, and Infrastructure | 9.4 Upgrade infrastructure for sustainability | Advancing environmentally sound technologies for metal recovery | Implementation of new metal recovery technologies, reduction in environmental impact |
| 12. Responsible Consumption and Production | 12.2 Achieve sustainable management and efficient use | Efficient recovery and recycling of critical metals to minimize resource depletion | Amount of metals recovered, reduction in primary metal extraction, resource efficiency ratio |

| | | | |
|---|---|---|---|
| | of natural resources | | |
| | 12.4 Achieve environmentally sound management of chemicals and all wastes | Safe recycling processes to manage metal wastes and reduce environmental pollution | Compliance with environmental regulations, reduction in hazardous waste, effectiveness of recycling methods |
| | 12.5 Substantially reduce waste generation | Improved recycling and recovery of critical metals | Reduction in metal waste, recycling rates of critical metals |
| | 12.a Support developing countries to strengthen their scientific and technological capacity | Developing innovative recycling technologies that can be shared globally | Number of technology transfers to developing countries, capacity-building initiatives, collaborative projects |
| | 12.8 Ensure that people everywhere have an awareness of sustainable development and lifestyles in harmony with nature | Raising awareness of the importance of metal recycling and sustainable resource use | Outreach and educational initiatives, public awareness campaigns, dissemination of research findings |
| 13. Climate Action | 13.2 Integrate climate change measures | Reduction of greenhouse gas emissions through less mining | Reduction in CO2 emissions, comparison of emissions from recycling vs. mining |
| 14. Life Below Water | 14.1 Prevent marine pollution | Prevention of heavy metal release into | Metal concentrations in marine ecosystems, the |

| | | | |
|---|---|---|---|
| | | marine environments | effectiveness of metal recovery methods |
| 15. Life on Land | 15.1 Ensure sustainable use of terrestrial ecosystems | Preventing land degradation through effective metal recovery | The land area impacted by mining; the amount of land rehabilitated |

## 6.3. Final Assessment

The topic presented in this dissertation is of significant interest due to its relevance to the field of metal recovery and the potential for sustainable resource circulation. The research highlights the possibility of continuously recycling planetary resources without depleting them. Still, this field is challenging, requiring substantial patience and time to achieve viable results. Given more time, further exploration of this subject could profit valuable findings for metal separation.

# 7. References


[1] E. ; S. R. ; E. M. ; M. G. ; N. T. ; H. R. , Eds. van der Voet, "Environmental Risks and Challenges of Anthropogenic Metals Flows and Cycles," UNEP DTIE, Sustainable Consumption and Production Branch.

[2] S. J. R. Vargas, H. Passos, N. Schaeffer, and J. A. P. Coutinho, "Integrated Leaching and Separation of Metals Using Mixtures of Organic Acids and Ionic Liquids," *Molecules*, vol. 25, no. 23, 2020, doi: 10.3390/molecules25235570.

[3] T. E. Graedel *et al.*, "What Do We Know About Metal Recycling Rates?," *J Ind Ecol*, vol. 15, Jun. 2011, doi: 10.1111/j.1530-9290.2011.00342.x.

[4] C. Hagelüken, J. U. Lee-Shin, A. Carpentier, and C. Heron, "The EU Circular Economy and Its Relevance to Metal Recycling," *Recycling*, vol. 1, no. 2, pp. 242–253, 2016, doi: 10.3390/recycling1020242.

[5] European Comission, "ANNEXES to the Proposal for a Regulation of the European Parliament and of the Council establishing a framework for ensuring a secure and sustainable supply of critical raw materials and amending Regulations," 2023.

[6] F.-W. Wellmer and C. Hagelüken, "The Feedback Control Cycle of Mineral Supply, Increase of Raw Material Efficiency, and Sustainable Development," *Minerals*, vol. 5, no. 4, pp. 815–836, 2015, doi: 10.3390/min5040527.

[7] S. Bobba, S. Carrara, J. Huisman, F. Mathieux, C. Pavel, and I. European Commission. Directorate-General for Internal Market, *Critical raw materials for strategic technologies and sectors in the EU : a foresight study*.

[8] N. Schaeffer, H. Passos, I. Billard, N. Papaiconomou, and J. A. P. Coutinho, "Recovery of metals from waste electrical and electronic equipment (WEEE) using unconventional solvents based on ionic liquids," *Crit Rev Environ Sci Technol*, vol. 48, no. 13–15, pp. 859–922, Aug. 2018, doi: 10.1080/10643389.2018.1477417.

[9] F. O. Ongondo, I. D. Williams, and T. J. Cherrett, "How are WEEE doing? A global review of the management of electrical and electronic wastes," *Waste Management*, vol. 31, no. 4, pp. 714–730, Apr. 2011, doi: 10.1016/J.WASMAN.2010.10.023.

[10] I. Smout, J. Ye, and S. Kayaga, "Regulating for e-waste in China: Progress and challenges," *Proceedings of The Institution of Civil Engineers-municipal*

*Engineer - PROC INST CIVIL ENG MUNIC ENG*, vol. 162, pp. 79–85, Jun. 2009, doi: 10.1680/muen.2009.162.2.79.

[11] Z. Sun *et al.*, "Toward Sustainability for Recovery of Critical Metals from Electronic Waste: The Hydrochemistry Processes," *ACS Sustain Chem Eng*, vol. 5, no. 1, pp. 21–40, Jan. 2017, doi: 10.1021/acssuschemeng.6b00841.

[12] A. M. Wilson, P. J. Bailey, P. A. Tasker, J. R. Turkington, R. A. Grant, and J. B. Love, "Solvent extraction: the coordination chemistry behind extractive metallurgy," *Chem. Soc. Rev.*, vol. 43, no. 1, pp. 123–134, 2014, doi: 10.1039/C3CS60275C.

[13] A. Tuncuk, V. Stazi, A. Akcil, E. Y. Yazici, and H. Deveci, "Aqueous metal recovery techniques from e-scrap: Hydrometallurgy in recycling," *Miner Eng*, vol. 25, no. 1, pp. 28–37, 2012, doi: https://doi.org/10.1016/j.mineng.2011.09.019.

[14] J. Cui and L. Zhang, "Metallurgical recovery of metals from electronic waste: A review," *J Hazard Mater*, vol. 158, no. 2, pp. 228–256, 2008, doi: https://doi.org/10.1016/j.jhazmat.2008.02.001.

[15] M. M. Theron and J. F. R. Lues, *Organic Acids and Food Preservation*. CRC Press, 2010. doi: 10.1201/9781420078435.

[16] A. Kumar, R. Shukla, and A. Venkatachalam, "Studies of corrosion and electrochemical behavior of some metals and brass alloy under different media," *Rasayan Journal of Chemistry*, vol. 6, pp. 12–14, Jun. 2013.

[17] A. Marins *et al.*, "Synthesis of Ni and rare earth metal (La, Pr, and Nd) oxides from spent Ni–MH batteries by selective precipitation with formic acid an investigation of photoluminescence properties," *Ionics (Kiel)*, vol. 26, Jun. 2020, doi: 10.1007/s11581-019-03158-3.

[18] R. Golmohammadzadeh, F. Rashchi, and E. Vahidi, "Recovery of lithium and cobalt from spent lithium-ion batteries using organic acids: Process optimization and kinetic aspects," *Waste Management*, vol. 64, pp. 244–254, 2017, doi: https://doi.org/10.1016/j.wasman.2017.03.037.

[19] R. Golmohammadzadeh, F. Faraji, and F. Rashchi, "Recovery of lithium and cobalt from spent lithium ion batteries (LIBs) using organic acids as leaching reagents: A review," *Resour Conserv Recycl*, vol. 136, pp. 418–435, 2018, doi: https://doi.org/10.1016/j.resconrec.2018.04.024.

[20] A. Pathak, M. Vinoba, and R. Kothari, “Emerging role of organic acids in leaching of valuable metals from refinery-spent hydroprocessing catalysts, and potential techno-economic challenges: A review,” *Crit Rev Environ Sci Technol*, vol. 51, no. 1, pp. 1–43, 2021, doi: 10.1080/10643389.2019.1709399.

[21] H. Al-Sheeha, M. Marafi, V. Raghavan, and M. S. Rana, “Recycling and Recovery Routes for Spent Hydroprocessing Catalyst Waste,” *Ind Eng Chem Res*, vol. 52, no. 36, pp. 12794–12801, Sep. 2013, doi: 10.1021/ie4019148.

[22] European Chemical Agency, “Oxalic acid.” Accessed: Jun. 27, 2024. [Online]. Available: https://echa.europa.eu/ registration-dossier/-/registered-dossier/14786/5/3/2

[23] International Agency for Research on Cancer, *Evaluation of Carcinogenic Risks to Humans. Chemical Agents and Related Occupations*. 2012.

[24] M. Rito-Palomares, “Practical application of aqueous two-phase partition to process development for the recovery of biological products,” *Journal of Chromatography B*, vol. 807, no. 1, pp. 3–11, 2004, doi: https://doi.org/10.1016/j.jchromb.2004.01.008.

[25] S. Amrhein, M.-L. Schwab, M. Hoffmann, and J. Hubbuch, “Characterization of aqueous two phase systems by combining lab-on-a-chip technology with robotic liquid handling stations,” *J Chromatogr A*, vol. 1367, pp. 68–77, Nov. 2014, doi: 10.1016/j.chroma.2014.09.042.

[26] M. G. Freire *et al.*, “Aqueous biphasic systems: a boost brought about by using ionic liquids,” *Chem. Soc. Rev.*, vol. 41, no. 14, pp. 4966–4995, 2012, doi: 10.1039/C2CS35151J.

[27] T. Welton, “Ionic liquids: a brief history,” *Biophys Rev*, vol. 10, no. 3, pp. 691–706, 2018, doi: 10.1007/s12551-018-0419-2.

[28] X. Zhao, P. Cai, C. Sun, and Y. Pan, “Application of ionic liquids in separation and analysis of carbohydrates: State of the art and future trends,” *TrAC Trends in Analytical Chemistry*, vol. 111, pp. 148–162, 2019, doi: https://doi.org/10.1016/j.trac.2018.12.008.

[29] S. P. M. Ventura, F. A. e Silva, M. V Quental, D. Mondal, M. G. Freire, and J. A. P. Coutinho, “Ionic-Liquid-Mediated Extraction and Separation Processes for Bioactive Compounds: Past, Present, and Future Trends,” *Chem Rev*, vol. 117, no. 10, pp. 6984–7052, May 2017, doi: 10.1021/acs.chemrev.6b00550.

[30] K. A. Kurnia, M. G. Freire, and J. A. P. Coutinho, “Effect of Polyvalent Ions in the Formation of Ionic-Liquid-Based Aqueous Biphasic Systems,” *J Phys Chem B*, vol. 118, no. 1, pp. 297–308, Jan. 2014, doi: 10.1021/jp411933a.

[31] M. Gras *et al.*, “Ionic-Liquid-Based Acidic Aqueous Biphasic Systems for Simultaneous Leaching and Extraction of Metallic Ions,” *Angew Chem Int Ed Engl*, vol. 57, no. 6, p. 1563—1566, Feb. 2018, doi: 10.1002/anie.201711068.

[32] M. C. Hespanhol, B. M. Fontoura, J. C. Quintão, and L. H. M. da Silva, “Extraction and purification of gold from raw acidic electronic leachate using an aqueous biphasic system,” *J Taiwan Inst Chem Eng*, vol. 115, pp. 218–222, Oct. 2020, doi: 10.1016/j.jtice.2020.10.027.

[33] N. Schaeffer *et al.*, “A HNO3-Responsive Aqueous Biphasic System for Metal Separation: Application towards CeIV Recovery,” *ChemSusChem*, vol. 14, no. 14, pp. 3018–3026, 2021, doi: https://doi.org/10.1002/cssc.202101149.

[34] G. Meyer, R. Schweins, T. Youngs, J.-F. Dufrêche, I. Billard, and M. Plazanet, “How Temperature Rise Can Induce Phase Separation in Aqueous Biphasic Solutions,” *J Phys Chem Lett*, vol. 13, no. 12, pp. 2731–2736, Mar. 2022, doi: 10.1021/acs.jpclett.2c00146.

[35] N. Schaeffer, G. Pérez-Sánchez, H. Passos, J. R. B. Gomes, N. Papaiconomou, and J. A. P. Coutinho, “Mechanisms of phase separation in temperature-responsive acidic aqueous biphasic systems,” *Physical Chemistry Chemical Physics*, vol. 21, no. 14, pp. 7462–7473, 2019, doi: 10.1039/c8cp07750a.

[36] N. Schaeffer *et al.*, “Mechanism of ionic-liquid-based acidic aqueous biphasic system formation,” *Physical Chemistry Chemical Physics*, vol. 20, no. 15, pp. 9838–9846, 2018, doi: 10.1039/c8cp00937f.

[37] V. Mogilireddy *et al.*, “Understanding the fundamentals of acid-induced ionic liquid-based aqueous biphasic system,” *Phys. Chem. Chem. Phys.*, vol. 20, no. 24, pp. 16477–16484, 2018, doi: 10.1039/C8CP02862A.

[38] Y. Kohno and H. Ohno, “Ionic liquid/water mixtures: from hostility to conciliation,” *Chem. Commun.*, vol. 48, no. 57, pp. 7119–7130, 2012, doi: 10.1039/C2CC31638B.

[39] Y. Kohno, S. Saita, Y. Men, J. Yuan, and H. Ohno, “Thermoresponsive polyelectrolytes derived from ionic liquids,” *Polym. Chem.*, vol. 6, no. 12, pp. 2163–2178, 2015, doi: 10.1039/C4PY01665C.

[40] O. Longeras, A. Gautier, K. Ballerat-Busserolles, and J.-M. Andanson, "Deep Eutectic Solvent with Thermo-Switchable Hydrophobicity," *ACS Sustain Chem Eng*, vol. 8, no. 33, pp. 12516–12520, Aug. 2020, doi: 10.1021/acssuschemeng.0c03478.

[41] S. Kumar, V. Aswal, A. Naqvi, and P. Goyal, "Cloud Point Phenomenon in Ionic Micellar Solutions: A SANS Study," *Langmuir*, vol. 17, Jun. 2001, doi: 10.1021/la001215p.

[42] D. Dong, J. B. Hooper, and D. Bedrov, "Structural and Dynamical Properties of Tetraalkylammonium Bromide Aqueous Solutions: A Molecular Dynamics Simulation Study Using a Polarizable Force Field," *J Phys Chem B*, vol. 121, no. 18, pp. 4853–4863, May 2017, doi: 10.1021/acs.jpcb.7b01032.

[43] S. Saita, Y. Kohno, and H. Ohno, "Detection of small differences in the hydrophilicity of ions using the LCST-type phase transition of an ionic liquid–water mixture," *Chem. Commun.*, vol. 49, no. 1, pp. 93–95, 2013, doi: 10.1039/C2CC37006A.

[44] V. A. Azov, K. S. Egorova, M. M. Seitkalieva, A. S. Kashin, and V. P. Ananikov, "'Solvent-in-salt' systems for design of new materials in chemistry, biology and energy research," *Chem. Soc. Rev.*, vol. 47, no. 4, pp. 1250–1284, 2018, doi: 10.1039/C7CS00547D.

[45] N. Schaeffer, G. Pérez-Sánchez, H. Passos, J. R. B. Gomes, N. Papaiconomou, and J. A. P. Coutinho, "Mechanisms of phase separation in temperature-responsive acidic aqueous biphasic systems," *Phys. Chem. Chem. Phys.*, vol. 21, no. 14, pp. 7462–7473, 2019, doi: 10.1039/C8CP07750A.

[46] R. Lommelen, T. Vander Hoogerstraete, B. Onghena, I. Billard, and K. Binnemans, "Model for Metal Extraction from Chloride Media with Basic Extractants: A Coordination Chemistry Approach," *Inorg Chem*, vol. 58, no. 18, pp. 12289–12301, Sep. 2019, doi: 10.1021/acs.inorgchem.9b01782.

[47] A. R. F. Carreira *et al.*, "Factors driving metal partition in ionic liquid-based acidic aqueous biphasic systems," *Sep Purif Technol*, vol. 299, Oct. 2022, doi: 10.1016/j.seppur.2022.121720.

[48] ChemAxon, "ChemAxon." Accessed: Jun. 24, 2024. [Online]. Available: https://chemaxon.com/products/marvin

[49] S. P. M. Ventura, C. M. S. S. Neves, M. G. Freire, I. M. Marrucho, J. Oliveira, and J. A. P. Coutinho, "Evaluation of Anion Influence on the Formation and

Extraction Capacity of Ionic-Liquid-Based Aqueous Biphasic Systems," *J Phys Chem B*, vol. 113, no. 27, pp. 9304–9310, Jul. 2009, doi: 10.1021/jp903286d.

[50] C. M. S. S. Neves, S. P. M. Ventura, M. G. Freire, I. M. Marrucho, and J. A. P. Coutinho, "Evaluation of cation influence on the formation and extraction capability of ionic-liquid-based aqueous biphasic systems," *J Phys Chem B*, vol. 113, no. 15, p. 5194—5199, Apr. 2009, doi: 10.1021/jp900293v.

[51] G. Tubio, L. Malpiedi, B. Nerli, and G. Picó, "Liquid−Liquid Equilibria of Aqueous Two-Phase Systems Containing Poly(ethylene glycols) of Different Molecular Weight and Sodium Citrate," *Journal of Chemical and Engineering Data - J CHEM ENG DATA*, vol. 51, Jul. 2005, doi: 10.1021/je050332p.

[52] S. M. Waziri, B. F. Abu-Sharkh, and S. A. Ali, "The effect of pH and salt concentration on the coexistence curves of aqueous two-phase systems containing a pH responsive copolymer and polyethylene glycol," *Fluid Phase Equilib*, vol. 205, no. 2, pp. 275–290, 2003, doi: https://doi.org/10.1016/S0378-3812(02)00297-2.

[53] M. T. Zafarani-Moattar and A. A. Hamidi, "Liquid−Liquid Equilibria of Aqueous Two-Phase Poly(ethylene glycol)−Potassium Citrate System," *J Chem Eng Data*, vol. 48, no. 2, pp. 262–265, Mar. 2003, doi: 10.1021/je0255527.

[54] T. Graber and M. Taboada, "Liquid−Liquid Equilibrium of the Poly(ethylene glycol) + Sodium Nitrate + Water System at 298.15 K," *Journal of Chemical and Engineering Data - J CHEM ENG DATA*, vol. 45, Jul. 2000, doi: 10.1021/je990225t.

[55] M. T. Zafarani-Moattar and E. Nemati-Kande, "Thermodynamic studies on the complete phase diagram of aqueous two phase system containing polyethylene glycol dimethyl ether 2000 and di-potassium hydrogen phosphate at different temperatures," *Calphad*, vol. 35, no. 2, pp. 165–172, 2011, doi: https://doi.org/10.1016/j.calphad.2011.02.004.

[56] J. C. Merchuk, B. A. Andrews, and J. A. Asenjo, "Aqueous two-phase systems for protein separation: Studies on phase inversion," *J Chromatogr B Biomed Sci Appl*, vol. 711, no. 1, pp. 285–293, 1998, doi: https://doi.org/10.1016/S0378-4347(97)00594-X.

[57] K. E. Gutowski *et al.*, "Controlling the Aqueous Miscibility of Ionic Liquids: Aqueous Biphasic Systems of Water-Miscible Ionic Liquids and Water-Structuring Salts for Recycle, Metathesis, and Separations," *J Am Chem Soc*, vol. 125, no. 22, pp. 6632–6633, Jun. 2003, doi: 10.1021/ja0351802.

[58] N. Schaeffer *et al.*, "Synergistic Aqueous Biphasic Systems: A New Paradigm for the 'One-Pot' Hydrometallurgical Recovery of Critical Metals," *ACS Sustain Chem Eng*, vol. 7, no. 1, pp. 1769–1777, Jan. 2019, doi: 10.1021/acssuschemeng.8b05754.

[59] United Nations, "THE 17 GOALS," https://sdgs.un.org/goals. Accessed: Jun. 29, 2024. [Online]. Available: https://sdgs.un.org/goals

# Appendix A – Solubility curves data

## A.1 Experimental solubility data for systems composed of $[P_{44414}]Cl$ + acid + $H_2O$

The experimental mass fraction percentage (m%) data for the phase diagrams of the systems composed of $[P_{44414}]Cl$ + acid + $H_2O$ are presented in Table A 1 to Table A 5.

*Table A1 - Experimental mass fraction percentage data for the systems composed of $[P_{44414}]Cl$ + $C_6H_8O_7$ + $H_2O$ and 298 K and 323 K and atmospheric pressure.*

| $[C_6H_8O_7]$ M = 192.124 g.mol$^{-1}$ | | | |
|---|---|---|---|
| 298 K | | 323 K | |
| [IL] / m% | [acid] / m% | [IL] / m% | [acid] / %m |
| 73.76 | 4.45 | 77.64 | 1.51 |
| 70.91 | 5.33 | 71.99 | 3.34 |
| 66.34 | 8.78 | 65.16 | 4.69 |
| 56.82 | 9.28 | 61.62 | 5.91 |

*Table A2 - Experimental mass fraction data for the systems composed of $[P_{44414}]Cl$ + $C_3H_6O_3$ + $H_2O$ at 298 K and atmospheric pressure.*

| $[C_3H_6O_3]$ M = 90.08 g.mol$^{-1}$ | |
|---|---|
| [IL] / m% | [acid] / m% |
| 76.22 | 4.13 |
| 69.91 | 5.81 |
| 59.25 | 11.62 |
| 55.08 | 13.37 |
| 51.51 | 15.08 |

*Table A3 - Experimental mass fraction percentage data for the systems composed of $[P_{44414}]Cl + C_3H_6O_2 + H_2O$ at 298 K and atmospheric pressure.*

| $[C_3H_6O_2]$ M = 74.08 g.mol$^{-1}$ | | | |
|---|---|---|---|
| [IL] / m% | [acid] / m% | [IL] / m% | [acid] / m% |
| 64.1 | 7.5 | 27.0 | 13.8 |
| 53.8 | 10.1 | 25.9 | 14.0 |
| 49.0 | 10.6 | 24.6 | 13.6 |
| 45.7 | 10.7 | 22.5 | 13.7 |
| 42.5 | 11.3 | 22.2 | 13.7 |
| 40.4 | 11.9 | 21.8 | 13.7 |
| 38.8 | 12.3 | 21.2 | 13.8 |
| 37.2 | 12.9 | 20.8 | 13.9 |
| 35.2 | 13.5 | 20.3 | 14.1 |
| 33.6 | 13.7 | 19.7 | 14.1 |
| 31.9 | 14.0 | 18.6 | 14.2 |
| 29.5 | 13.8 | 18.3 | 14.3 |
| 28.4 | 13.8 | 15.4 | 15.1 |
| 27.7 | 13.7 | 14.7 | 15.5 |

*Table A4 - Experimental mass fraction percentage data for the systems composed of $[P_{44414}]Cl$ + $C_4H_8O_2$ + $H_2O$ at 298 K and atmospheric pressure.*

| $[C_4H_8O_2]$ M = 88.11 g.mol$^{-1}$ | | | |
|---|---|---|---|
| [IL] / m% | [acid] / m% | [IL] / m% | [acid] / m% |
| 68.33 | 5.77 | 18.59 | 7.79 |
| 64.09 | 7.57 | 17.26 | 7.32 |
| 57.04 | 9.24 | 17.14 | 7.43 |
| 55.95 | 9.47 | 16.39 | 7.31 |
| 52.72 | 9.64 | 15.86 | 7.24 |
| 51.89 | 10.05 | 14.75 | 6.80 |
| 50.02 | 10.15 | 14.38 | 7.26 |
| 47.50 | 10.61 | 14.04 | 6.71 |
| 46.30 | 10.73 | 12.88 | 6.91 |
| 45.13 | 11.01 | 12.65 | 6.52 |
| 43.13 | 11.05 | 11.61 | 6.45 |
| 40.93 | 11.24 | 11.54 | 6.38 |
| 38.20 | 11.10 | 10.86 | 6.27 |
| 37.96 | 10.84 | 10.21 | 6.08 |
| 36.21 | 11.20 | 10.06 | 6.01 |
| 36.01 | 11.09 | 9.60 | 6.18 |
| 34.98 | 11.32 | 9.54 | 6.01 |
| 33.92 | 11.57 | 8.53 | 5.95 |
| 33.02 | 11.36 | 8.48 | 5.58 |
| 30.87 | 11.76 | 8.03 | 5.65 |
| 25.94 | 10.48 | 7.50 | 5.62 |
| 25.38 | 9.11 | 7.33 | 5.51 |
| 22.91 | 8.61 | 6.69 | 5.36 |
| 21.07 | 8.27 | 6.19 | 5.25 |

*Table A5 - Experimental mass fraction percentage data for the systems composed of $[P_{44414}]Cl$ + $CH_2O_2$ + $H_2O$ at 298 K and atmospheric pressure.*

| $[CH_2O_2]$ M = 46.03 g.mol$^{-1}$ | | | |
|---|---|---|---|
| [IL] / m% | [acid] / m% | [IL] / m% | [acid] / m% |
| 58.30 | 6.50 | 22.56 | 11.11 |
| 51.45 | 7.41 | 21.37 | 11.43 |
| 46.14 | 8.09 | 20.19 | 11.45 |
| 41.96 | 8.73 | 18.75 | 11.74 |
| 37.88 | 10.09 | 17.61 | 11.79 |
| 34.37 | 10.37 | 16.80 | 11.97 |
| 31.93 | 10.97 | 15.58 | 11.63 |
| 28.66 | 11.36 | 14.95 | 11.94 |
| 25.86 | 11.49 | 14.37 | 11.98 |
| 24.65 | 11.43 | 13.85 | 12.03 |

## A.2 Experimental solubility data for systems composed of $[P_{44414}]Cl$ + salt + $H_2O$

The experimental mass fraction percentage data for the phase diagrams of the systems composed of $[P_{44414}]Cl$ + salt + $H_2O$ are presented in Table A 6 to Table A 8.

*Table A6 - Experimental mass fraction percentage data for the systems composed of $[P_{44414}]Cl$ + $K_3C_6H_5O_7$ + $H_2O$ at 298 K and atmospheric pressure.*

| $[K_3C_6H_5O_7]$ M = 306.40 g.mol$^{-1}$ | | | |
|---|---|---|---|
| [IL] / m% | [acid] / m% | [IL] / m% | [acid] / m% |
| 77.29 | 1.38 | 16.57 | 15.72 |
| 41.99 | 5.00 | 16.20 | 15.86 |
| 39.16 | 5.47 | 15.51 | 16.48 |
| 37.04 | 5.99 | 15.64 | 16.95 |
| 32.27 | 7.84 | 15.04 | 17.55 |
| 28.99 | 9.10 | 13.81 | 18.48 |
| 27.28 | 9.86 | 12.22 | 19.97 |
| 25.83 | 10.75 | 10.84 | 21.00 |
| 22.63 | 11.90 | 10.46 | 21.73 |
| 21.31 | 12.58 | 9.51 | 22.51 |
| 20.52 | 13.08 | 9.00 | 24.16 |
| 19.74 | 13.46 | 7.72 | 26.15 |
| 19.25 | 13.80 | 6.37 | 28.39 |
| 18.58 | 14.22 | 4.30 | 30.92 |
| 17.84 | 14.73 | 3.51 | 33.04 |
| 17.26 | 15.13 | 2.82 | 39.78 |

*Table A7 - Experimental mass fraction percentage data for the systems composed of $[P_{44414}]Cl$ + $NaC_2H_3O_2$ + $H_2O$ at 298 K and atmospheric pressure.*

| $[NaC_2H_3O_2]$ M = 82.03 g.mol$^{-1}$ | | | |
|---|---|---|---|
| [IL] / m% | [acid] / m% | [IL] / m% | [acid] / m% |
| 75.63 | 1.23 | 19.37 | 13.48 |
| 66.49 | 2.88 | 18.39 | 13.89 |
| 56.64 | 4.21 | 17.29 | 14.39 |
| 50.01 | 5.43 | 16.66 | 14.66 |
| 43.46 | 6.71 | 15.68 | 15.16 |
| 37.98 | 7.98 | 14.18 | 15.79 |
| 35.44 | 8.61 | 13.33 | 16.25 |
| 33.43 | 9.06 | 12.56 | 16.68 |
| 31.56 | 9.51 | 11.95 | 17.07 |
| 29.17 | 10.25 | 10.97 | 17.66 |
| 26.82 | 10.96 | 10.55 | 17.86 |
| 22.89 | 12.09 | 9.95 | 18.23 |
| 21.86 | 12.45 | 9.54 | 18.52 |
| 20.37 | 13.04 | | |

*Table A8 - Experimental mass fraction percentage data for the systems composed of $[P_{44414}]Cl$ + $NaCHO_2$ + $H_2O$ and 298 K and atmospheric pressure.*

| [$NaCHO_2$] M = 68.01 g.mol$^{-1}$ | | | | | |
|---|---|---|---|---|---|
| [IL] / m% | [acid] / m% | [IL] / m% | [acid] / m% | [IL] / m% | [acid] / m% |
| 78.92 | 1.11 | 22.80 | 9.23 | 8.98 | 14.29 |
| 72.44 | 2.06 | 22.27 | 9.31 | 8.17 | 14.72 |
| 62.67 | 2.72 | 21.64 | 9.65 | 7.75 | 14.46 |
| 57.92 | 3.40 | 18.36 | 10.49 | 7.11 | 14.66 |
| 53.86 | 4.30 | 17.32 | 10.48 | 6.89 | 14.56 |
| 45.24 | 4.40 | 17.16 | 10.60 | 5.91 | 15.23 |
| 42.92 | 4.64 | 16.79 | 10.72 | 5.76 | 15.29 |
| 39.91 | 4.94 | 16.47 | 10.91 | 5.59 | 15.73 |
| 39.00 | 5.28 | 15.62 | 11.24 | 4.97 | 16.05 |
| 37.52 | 5.75 | 15.12 | 11.48 | 4.76 | 15.78 |
| 32.23 | 7.26 | 14.17 | 12.14 | 4.57 | 15.80 |
| 29.56 | 7.97 | 14.13 | 12.92 | 4.01 | 15.91 |
| 28.14 | 8.19 | 10.66 | 13.99 | 3.92 | 16.06 |
| 27.38 | 8.33 | 9.94 | 14.03 | 3.79 | 16.10 |
| 23.68 | 9.00 | 9.41 | 14.26 | | |

## A.3 Experimental solubility data for systems composed of $[P_{44414}]Cl$ + acid + salt + $H_2O$

The experimental mass fraction percentage data for the phase diagrams of the systems composed of $[P_{44414}]Cl$ + acid + salt + $H_2O$ are presented in Table A 9 to Table A 10.

*Table A9 - Experimental mass fraction data for the systems composed of $[P_{44414}]Cl$ + $C_6H_8O_7$ + $K_3C_6H_5O_7$ (5 m%) + $H_2O$ and 298 K and atmospheric pressure.*

| $[C_6H_8O_7]$ M = 192.12 g.mol$^{-1}$ | | | |
|---|---|---|---|
| [IL] / m% | [acid] / m% | [IL] / m% | [acid] / m% |
| 45.99 | 0.75 | 27.27 | 6.46 |
| 44.07 | 1.50 | 26.79 | 6.50 |
| 42.15 | 2.83 | 26.35 | 6.53 |
| 40.74 | 3.89 | 24.24 | 6.74 |
| 39.28 | 4.47 | 23.36 | 6.75 |
| 37.78 | 4.88 | 22.76 | 6.71 |
| 36.78 | 5.06 | 22.49 | 6.73 |
| 35.94 | 5.65 | 19.36 | 6.87 |
| 34.39 | 5.62 | 17.58 | 6.86 |
| 33.40 | 5.92 | 16.49 | 6.90 |
| 32.35 | 5.91 | 15.50 | 6.81 |
| 31.84 | 5.97 | 14.60 | 6.73 |
| 31.35 | 6.06 | 13.63 | 6.62 |
| 30.68 | 6.19 | 12.26 | 6.68 |
| 29.84 | 6.19 | 11.60 | 6.50 |
| 29.43 | 6.28 | 11.07 | 6.45 |
| 28.91 | 6.30 | 10.26 | 6.31 |

*Table A10 - Experimental mass fraction percentage data for the systems composed of $[P_{44414}]Cl$ + 5 m% $C_6H_8O_7$ + $K_3C_6H_5O_7$ + $H_2O$ and 298 K and atmospheric pressure.*

| $[K_3C_6H_5O_7]$ M = 306.40 g.mol$^{-1}$ | | | |
|---|---|---|---|
| [IL] / m% | [acid] / m% | [IL] / m% | [acid] / m% |
| 44.07 | 1.50 | 26.35 | 6.53 |
| 42.15 | 2.83 | 24.24 | 6.74 |
| 40.74 | 3.89 | 23.36 | 6.75 |
| 39.28 | 4.47 | 22.76 | 6.71 |
| 37.78 | 4.88 | 22.49 | 6.73 |
| 36.78 | 5.06 | 19.36 | 6.87 |
| 35.94 | 5.65 | 17.58 | 6.86 |
| 34.39 | 5.62 | 16.49 | 6.90 |
| 33.40 | 5.92 | 15.50 | 6.81 |
| 32.35 | 5.91 | 14.60 | 6.73 |
| 31.84 | 5.97 | 13.63 | 6.62 |
| 31.35 | 6.06 | 12.26 | 6.68 |
| 30.68 | 6.19 | 11.60 | 6.50 |
| 29.84 | 6.19 | 11.07 | 6.45 |
| 29.43 | 6.28 | 10.26 | 6.31 |
| 28.91 | 6.30 | 5.97 | 47.11 |
| 27.27 | 6.46 | 5.96 | 35.87 |

# Appendix B – Copper calibration curve

Figure B1 shows the calibration curve (concentration *vs.* absorbance) of copper.

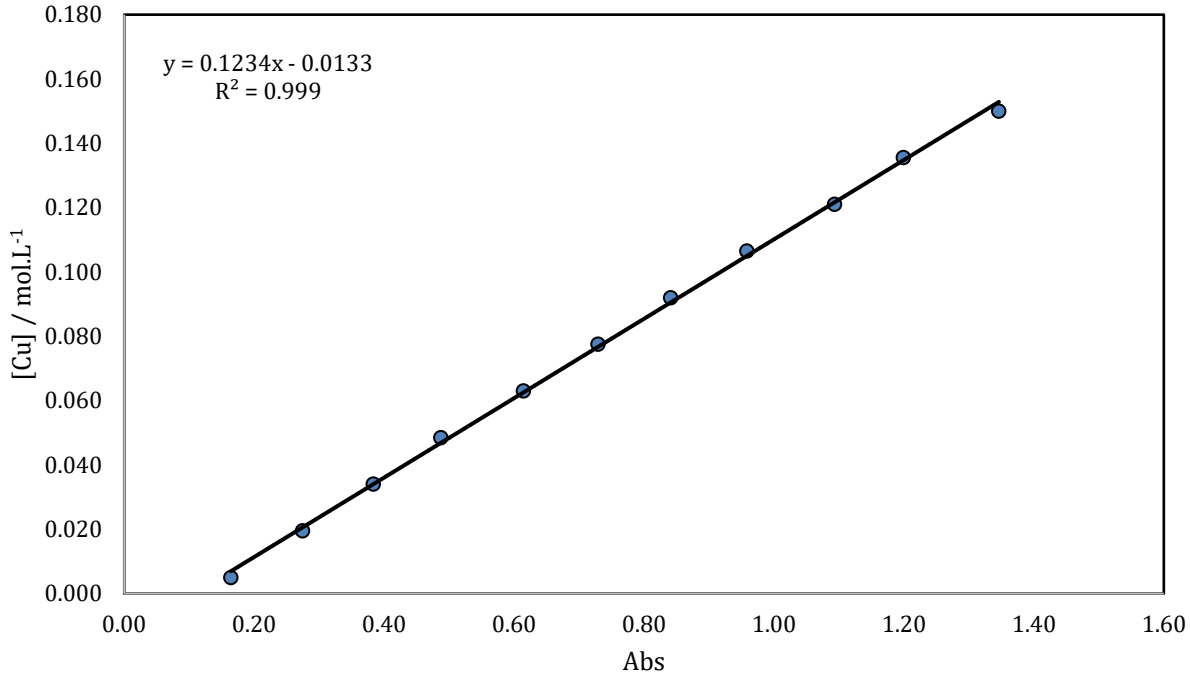



*Figure B10 - Calibration curve for copper at λ = 817 nm.*